Stabilized High-Order Discontinuous Galerkin Methods for Convection-Diffusion-Reaction equations

Faraz Khatami
Supervisor: Professor. Ramon Codina

International Center for Numerical Methods in Engineering (CIMNE)
Escola Tecnica Suprior d'Enginyers de Camins, Canals i Ports de Barcelona

Universitat Politècnica De Catalunya

A thesis submitted for the degree of

Master of Science in Computational Mechanics

June 2011

1. Reviewer:

2. Reviewer:

Day of the defense:

Signature from coordinator of the MSc program:

Abstract

A stabilized Discontinuous Galerkin (DG) formulation has been proposed for Convection Diffusion Reaction (CDR) equations using high order approximations. Let Ω be a bounded polygonal domain in $\mathbb{R}^d$ with boundary $\partial\Omega$, the strong form of the CDR boundary value problem is the following:

$$\begin{aligned} \mathcal{L}u := -k\Delta u + \boldsymbol{a}\cdot\nabla u + su = f \qquad & in\,\Omega, \\ u = 0 \qquad & on\,\partial\Omega \end{aligned}$$

using Discontinuous Galerkin (DG) interpolation for the unknown u. Here it is considered that the diffusion coefficient $k > 0$, the convection velocity $\boldsymbol{a} \in \mathbb{R}^d$, and reaction coefficient $s \geq 0$ are all constant.

Our objective is two-fold. Firstly, we derive the discontinuous Galerkin approximation from a hybrid form of the problem and, secondly, we motivate the introduction of additional stabilization terms based on the variational multiscale framework.

Let $T_h = \{K\}$ be a regular finite element partition of Ω. The hybrid formulation from which we start consists of finding u_h, its traces on the element edges γ_h, and its fluxes on the element boundaries λ_h such that

$$\begin{aligned} &\sum_K B_K\left(u_h, v_h\right) - \sum_K \langle \lambda_h, v_h\rangle_{\partial K} = \sum_K L_K\left(v_h\right), \\ &\sum_K \langle \kappa_h, \lambda_h\rangle_{\partial K} = 0, \\ &\sum_K \langle \mu_h, \gamma_h - u_h\rangle_{\partial K} = 0 \end{aligned}$$

for all test functions v_h, κ_h, and μ_h in the appropriate finite element spaces. B_K and L_K are the bilinear and linear form associated to the variational formulation of the problem defined within each element. This hybrid formulation would require compatibility conditions between these spaces, which

could be written in the form of inf-sup conditions. However, instead of interpolating the traces and the fluxes, they have been determined using Taylor expansions to approximate the fluxes and then imposing continuity of the unknown to compute the traces. The final result is a problem posed only in terms of the unknown u_h defined in the interior of the element domains.

The resulting discontinuous Galerkin formulation turns out to be very classical. Weak continuity of u_h across elements is enforced through an interior penalty method, which appears in a natural way, whereas terms that ensure adjoint consistency in the purely diffusive case arise naturally, without the need to introduce them in an ad-hoc manner. The only aspect that differs from classical approaches is the term that enforces continuity in the direction of a when $k \to 0$. The final method we propose is

$$\sum_K B_K\left(u_h, v_h\right) + \frac{k}{\delta}\sum_E \left\langle [\![\boldsymbol{n}u_h]\!], [\![\boldsymbol{n}v_h]\!]\right\rangle_E + \frac{\delta}{2}\sum_E \left\langle [\![\boldsymbol{n}\cdot\nabla v_h]\!], [\![\boldsymbol{n}\cdot\boldsymbol{a}u_h]\!]\right\rangle_E$$
$$-\sum_E \left\langle [\![\boldsymbol{n}u_h]\!], k\left\{\nabla v_h\right\}\right\rangle_E - \sum_E \left\langle [\![\boldsymbol{n}v_h]\!], k\left\{\nabla u_h\right\}\right\rangle_E = \sum_K L_K\left(v_h\right)$$

where $[\![\cdot]\!]$ and $\{\cdot\}$ are the jump and the average operators defined on the edges E, respectively, and δ is the so-called penalty parameter which is proportional to the mesh size h whose interpretation have been provided. The symbol $\langle f, g\rangle_\omega$ has been used to denote the integral of fg in a region ω.

Some simple numerical examples have been carried out using the developed DG formulation in the case of convection-dominated CDR problem which have been compared to the Continuous Galerkin (CG) results obtained for the same problem. It has been shown that the results obtained using the DG method are strongly dependent on the penalty parameter δ. Suppose $\delta = \alpha h$, if $\alpha \to 0$, the formulation will enforce strongly the continuity when k is fixed. For critical values of penalty parameter when $\alpha \to \alpha_c$ (with an interpretation of $\alpha_c = 0.5$) excessive continuity in the direction of a will be enforced when $k \to 0$. This already anticipates that the same stability problems as for the continuous Galerkin approximation may be encountered in these limit situations.

To overcome them, a possibility is to use the same stabilization strategy for discontinuous interpolations as for continuous ones. The proposed stabilized formulation can be motivated from the variational multiscale concept. If u_h is split into a resolvable component, still denoted u_h, and an unresolvable one, and the latter is approximated in terms of the former (for example using a Fourier argument), the introduction of the stabilizing term

$$\sum_K \langle \tau \left(\boldsymbol{a} \cdot \nabla v_h + k \Delta v_h - s v_h \right), \boldsymbol{a} \cdot \nabla u_h - k \Delta u_h + s u_h - f \rangle_K$$

can be motivated, where τ is the stabilization parameter that appears also in classical stabilized finite element methods. From several numerical examples the benefits of adding stabilization to the original discontinuous Galerkin formulation have been shown. Without this term, the solution exhibits a strong dependence on the parameter α that enforces weak continuity of the unknown. Adding the stabilization term the solution is virtually insensitive to this parameter. From the analytical point of view, these results are explained by the dependence of the stability and convergence bounds on α, which explode as continuity of the unknown is excessively enforced and no additional stabilization is added.

Acknowledgements

First, I would like to thank my advisor Prof. Ramon Codina for letting me the opportunity to work on this project, for his constant support, and for his always insightful guidance. I admire how he explains the topics deeply and such completely. His ideas were always motivational especially during the times when I believed to be near a dead end.

I would like to thank Prof. Ghader Rezazadeh, my advisor back in my BSc studies, who recognized my potential in research and gave me the opportunity to do research in his group during my bachelors. A period when I could get involved in various computational projects, and got the confidence to apply for such prestigious master program.

And of course, I am forever indebted to my parents for their unwavering support in my life.

This project was made possible by support of European Union through the graduate program, Erasmus Mundus master of science in computational mechanics, coordinated by *international center for numerical methods in engineering* (*CIMNE*).

Contents

List of Figures

LIST OF FIGURES

1

Introduction

1.1 Problem statement

In this work finite element approximation of the Convection-Diffusion-Reaction (CDR) equation has been considered. Let Ω be a bounded polygonal domain in $\mathbb{R}^d$, the strong form of the CDR boundary value problem is the following:

$$\begin{aligned} \mathcal{L}u := -k\Delta u + \boldsymbol{a} \cdot \nabla u + su = f \qquad & in\, \Omega, \\ u = 0 \qquad & on\, \partial\Omega \end{aligned} \tag{1.1}$$

using Discontinuous Galerkin (DG) interpolation for the unknown u.

Here, the coefficient $k > 0$ is the (positive definite) and symmetric diffusion tensor, $\boldsymbol{a} \in \mathbb{R}^d$ the velocity field, and $s \geq 0$ is the reaction coefficient, which are all considered to be constant. Also, $\partial\Omega$ is the boundary on which Dirichlet boundary conditions are imposed. In Chapter 4, an application-based combustion problem governed by transient nonlinear reaction-convection-diffusion equation has been introduced in which more general boundaries including Neumann boundary conditions have been considered. Finally, it is assumed that the values of the coefficients $\mathbf{a}$, k and s are such that ensure wellposedness of 1.1.

1.2 State of the art

Convection-Diffusion-Reaction (CDR) equation models the transport and reaction of particles inside a physical system. These types of problems occur in mathematical modeling of wide range of applications such as heat and mass transfer, magneto-statics

and electro-statics, flow and transport in porous media problems related to petroleum and ground water applications etc. In applications, typically the size of the diffusion is much smaller than the size of the convective term i.e. the problem is convection-dominated or in terms of mesh Peclet number when $((|\boldsymbol{a}|\, h)/k) \gg 0$. Despite the apparent simplicity of the CDR equation, its numerical solution is still a challenge for convection dominated problems. It is well-known that, in case of dominant convection, conforming finite element methods perform poorly and usually globally polluted by spurious oscillations causing a severe loss of accuracy and stability. In order to get physically sound numerical approximations, stabilization strategies are required.

The word stabilization refers to all the extra terms added to the standard bilinear formulation of CDR of its Galerkin discretization in such way that consistency is preserved and numerical stability is enhanced. Using some notations introduced in chapter (2.1) and using the definitions provided in the same chapter for bilinear and linear forms of the CDR problem, the stabilized formulation written based on the variational form of the problem can be expressed as follows,

$$B(u_h, v_h) + S(u_h, v_h) = L(v_h) \tag{1.2}$$

where $S(u_h, v_h)$ is the stabilization term.

Various techniques have been proposed for the stabilization of CDR equations. Upwind techniques were introduced after the stabilization problem was identified as lack of diffusion in discrete solution. The solution proposed by upwind techniques consisted in adding numerical dissipation in the context of the finite difference method. One of the major contributions to this development was made by Christie *et al.* (16), who showed that using asymmetric test functions in a weighted residual finite element formulation a stabilization in one-dimensional case can be achieved. They found out the usual one-sided differences used for the convective term approximation in the finite difference method by suitable selection of the test functions. Heinrich *et al.* in (17) and Tababa in (18) developed two dimensional upwind finite element discretization following which many other upwind finite element strategies were introduced. The extra stabilization term introduced by upwind techniques to the original formulation is inconsistent and too much of numerical diffusion is introduced in formulation implying a loss of accuracy. Therefore the accuracy of the method is limited to first order approximations. Another shortcoming in upwind methods according to Brooks *et al.*

(13) is that non-consistent formulations can produce inaccurate or wrong solutions in presence of significant source term or time derivative (in case of transient CDR problem). Moreover, if the convection velocity $\boldsymbol{a}$ assumed to be skew directed in the domain partition, an excessive artificial diffusion can be observed perpendicular to the flow (crosswind diffusion).

Later on, a significant improvement was made by the method of Streamline Upwind PetrovGalerkin (SUPG) developed by (11, 12, 13) which considerably eliminates many difficulties that existed within the upwind method. Since the streamline diffusion added to the standard formulation in SUPG is consistent, stability is obtained with higher accuracy compared to upwind methods. In addition, SUPG introduces numerical diffusion only along the streamlines and hence does not perform any spurious crosswind diffusion. A generalization of SUPG was proposed for the Stokes problem in (15) which showed the potential of extending the idea to various applications. The SUPG method depends on a parameter called the stabilization parameter which is usually denoted by τ. This parameter also appears in the method of Galerkin least squares (GLS) which was introduced by Hughes *et al.* (14). They observed that the stabilization terms can be obtained by minimizing the square of the equation residual. Also, Douglas-Wang introduced their stabilization technique in (19) in the context of the Stokes problem which similar to GLS and SUPG is dependent on τ.

These methods were related to the introduction of bubble functions in (20, 21, 22), where it was shown that a choice of the bubble implies a choice of the stabilization parameter. A bubble function is, by definition, a function whose support is contained in a single element. For instance, in a two dimensional domain, increasing the order of approximation from first order to second order could be interpreted as adding three bubbles per element, that is, x^2, y^2, xy. The idea is based on the observation that adding bubbles to the finite element space and cutting them out from the Galerkin discretization is analogous to the addition of streamline diffusion to the standard formulation for stabilization. In this case rather than looking for a suitable τ, the question is how to define appropriate bubbles. The optimal bubble is given by the solution of a local subproblem driven by the residual (23), and is therefore named residual free. In 1995, Hughes (24) showed that stabilized methods could be derived from a Variational Multiscale (VMS) formulation. The key idea of the VMS method is based on a decomposition of the solution of a system of equations into coarse scales (directly simulated)

and fine scales (modeled or omitted in the numerical simulations). Then the effect of the fine scales is included in the coarse-scales, ultimately generating a subgrid model and/or stabilization term in the equations for the coarse scales. According to a comparison of different stabilization methods provided by R. Codina in (29), these methods can be identified as algebraic subgrid scales with a stabilization term $S(u_h, v_h)$ written as follows,

$$S(u_h, v_h) = \tau \left(\mathcal{R}(u_h), \mathcal{P}(v_h) \right)_\Omega \tag{1.3}$$

where τ is called the stabilization parameter. Also $\mathcal{R}(u_h)$ is the residual of the problem which using 1.1 can be written as,

$$\mathcal{R}(u_h) = \mathcal{L}(u_h) - f = -k\Delta u_h + \boldsymbol{a} \cdot \nabla u_h + s u_h - f \tag{1.4}$$

and $\mathcal{P}(v_h)$ is an operator acting on the test functions which, according to (29), for different methods is defined as follows,

$$\begin{cases} \mathcal{P}(v_h)|_{SUPG} = \boldsymbol{a} \cdot \nabla v_h \\ \mathcal{P}(v_h)|_{GLS} = \boldsymbol{a} \cdot \nabla v_h - k\Delta v_h + s v_h \\ \mathcal{P}(v_h)|_{VMS} = \boldsymbol{a} \cdot \nabla v_h + k\Delta v_h - s v_h \end{cases} \tag{1.5}$$

During the last decade, families of discontinuous Galerkin (DG) finite element methods have been proposed for the numerical solution of CDR problems. The increasing interest in DG methods is due to many attractive features they offer, in particular, their built-in stability, flexibility in implementation of unstructured meshes, allowing for hp-adaptive refinement, and local conservation of quantities. However, there are some shortcomings, namely, higher cost of DG methods in comparison with conforming finite elements due to duplication of side/face nodes, and edge integration. Though the problem with duplication of nodes for higher orders of interpolations is less important. Although the DG methods are felt to have advantages of robustness over conventional Galerkin methods for problems of hyperbolic type (3), yet their extension to elliptic problems is far less obvious. There has been recent interest in applying DG to elliptic problems for modeling of CDR problems (4, 5, 6). A unified framework have been proposed and analyzed by Arnold *et al.* in (9) to deal with elliptic problems. Also, a comparison of the performance of various schemes is analyzed in (25) from a practical point of view. Among various alternatives proposed for the treatment of second order derivatives are, the well-known Interior Penalty (IP) method proposed in (26), BR2 method in (1), and Local Discontinuous Galerkin (LDG) method proposed in (27).

1.3 Motivation of this work

One of the important characteristics of DG methods is their built-in stability through a penalty term in their formulation. A unified analysis of the DG methods carried out by Arnold *et al.* (9) show that the stabilization of DG methods via the inclusion of a penalty term is crucial such that without it convergence is degraded or lost. DG methods are felt to have good stability characteristics, however it has been observed that the vaunted robustness of the DG methods have been partially overstated, especially in the case of low order (linear case) approximations. In Hughes *et al.* (2), simple one-dimensional examples of pure advection and pure diffusion were shown to give rise to spurious oscillations which can demonstrate that stabilization of DG methods require further considerations.

The aim of this study is to extend the use of stabilization techniques based on scale-splitting to discontinuous Galerkin methods, where ad-hoc approaches are often employed. Also the relationship between existing and new methods is to be elucidated. To this end, Firstly, the discontinuous Galerkin approximation has been derived from a hybrid form of the problem and, secondly, an additional stabilization terms has been introduced based on the variational multiscale framework.

Let $T_h = \{K\}$ be a regular finite element partition of Ω. The hybrid formulation from which we start consists of finding u_h, its traces on the element edges γ_h, and its fluxes on the element boundaries λ_h such that

$$\sum_K B_K\left(u_h, v_h\right) - \sum_K \langle \lambda_h, v_h \rangle_{\partial K} = \sum_K L_K\left(v_h\right), \tag{1.6}$$

$$\sum_K \langle \kappa_h, \lambda_h \rangle_{\partial K} = 0, \tag{1.7}$$

$$\sum_K \langle \mu_h, \gamma_h - u_h \rangle_{\partial K} = 0 \tag{1.8}$$

for all test functions v_h, κ_h, and μ_h in the appropriate finite element spaces. B_K and L_K are the bilinear and linear form associated to the variational formulation of the problem defined within each element. This hybrid formulation would require compatibility conditions between these spaces, which could be written in the form of inf-sup conditions. However, instead of interpolating the traces and the fluxes, they have been determined using Taylor expansions to approximate the fluxes and then imposing continuity of the unknown to compute the traces. The final result is a problem posed only in

terms of the unknown u_h defined in the interior of the element domains. The resulting discontinuous Galerkin formulation turns out to be very classical. Weak continuity of u_h across elements is enforced through an interior penalty method, which appears in a natural way, whereas terms that ensure adjoint consistency in the purely diffusive case arise naturally, without the need to introduce them in an ad-hoc manner. The only aspect that differs from classical approaches is the term that enforces continuity in the direction of a when $k \to 0$. The final method we propose is

$$\sum_K B_K(u_h, v_h) + \frac{k}{\delta}\sum_E \langle [\![\boldsymbol{n}u_h]\!], [\![\boldsymbol{n}v_h]\!]\rangle_E + \frac{\delta}{2}\sum_E \langle [\![\boldsymbol{n}\cdot\nabla v_h]\!], [\![\boldsymbol{n}\cdot\boldsymbol{a}u_h]\!]\rangle_E \quad (1.9)$$
$$-\sum_E \langle [\![\boldsymbol{n}u_h]\!], k\{\nabla v_h\}\rangle_E - \sum_E \langle [\![\boldsymbol{n}v_h]\!], k\{\nabla u_h\}\rangle_E = \sum_K L_K(v_h)$$

where $[\![\cdot]\!]$ and $\{\cdot\}$ are the jump and the average operators defined on the edges E, respectively, and δ is a parameter proportional to the mesh size h whose interpretation have been provided. The symbol $\langle f, g\rangle_\omega$ has been used to denote the integral of fg in a region ω.

Suppose $\delta = \alpha h$, if $\alpha \to 0$, the formulation will enforce strongly the continuity when k is fixed. For critical values of penalty parameter when $\alpha \to \alpha_c$ (with an interpretation of $\alpha_c = 0.5$) excessive continuity in the direction of $\boldsymbol{a}$ will be enforced when $k \to 0$. This already anticipates that the same stability problems as for the continuous Galerkin approximation may be encountered in these limit situations.

To overcome them, a possibility is to use the same stabilization strategy for discontinuous interpolations as for continuous ones. The proposed stabilized formulation can be motivated from the variational multiscale concept. If u_h is split into a resolvable component, still denoted u_h, and an unresolvable one, and the latter is approximated in terms of the former (for example using a Fourier argument), the introduction of the stabilizing term

$$\sum_K \langle \tau(\boldsymbol{a}\cdot\nabla v_h + k\Delta v_h - s v_h), \boldsymbol{a}\cdot\nabla u_h - k\Delta u_h + s u_h - f\rangle_K \quad (1.10)$$

can be motivated, where τ is the stabilization parameter that appears also in classical stabilized finite element methods. From several numerical examples the benefits of adding stabilization to the original discontinuous Galerkin formulation have been shown. Without this term, the solution exhibits a strong dependence on the parameter α that enforces weak continuity of the unknown. Adding the stabilization term

the solution is virtually insensitive to this parameter. From the analytical point of view, these results are explained by the dependence of the stability and convergence bounds on α, which explode as continuity of the unknown is excessively enforced and no additional stabilization is added.

2

Variational Multiscale Methods

One of the early problems in Galerkin formulation of convection dominated CDR problems, is stability. Many stabilization techniques were developed starting with Upwind schemes after understanding the problem as a lack of diffusion in numerical solution of the problem. Other well-known techniques include Streamline Upwind Petrov-Galerkin (SUPG), Galerkin Least Squares (GLS), and Residual free Bubbles. In 1995, Hughes (24) showed that stabilized methods could be derived from a Variational Multiscale (VMS) formulation. The key idea of the VMS method is based on a decomposition of the solution of a system of equations into coarse scales (directly simulated) and fine scales (modeled or omitted in the numerical simulations). The effect of the fine scales on the coarse-scale dynamics is accounted for through local Greens function problems, ultimately responsible for the generation of a subgrid model and/or stabilization term in the equations for the coarse scales.

This chapter is divided into three parts: firstly the variational formulation of the CDR equations have been derived, in the second part scale splitting and subgrid scales modeling has been described within the context of VMS, and in the last part stabilized formulation of the CDR equations have been obtained considering continuous finite element approximation.

2.1 Variational formulation of the convection-diffusion-reaction equation

The strong form of CDR equation was expressed in 1.1. In order to obtain the variational formulation of the problem first let us introduce some functional settings considering a domain $\Omega \in \mathbb{R}^d$.

Letting A to be a domain of $\mathbb{R}^d$, the space of continuous function $C^0(A)$ is the set of all real valued functions which are continuous in A. if A is not a compact subset of $\mathbb{R}^d$, then $C^0(A)$ is the set of all real valued functions which are continuous and bounded in A. $C^m(A)$ is the subspace of $C^0(A)$ that have all the partial derivatives up to order m and these derivatives also belong to $C^0(A)$. The Lebesgue spaces $L^\infty(\Omega)$ is the set of all real valued functions defined almost everywhere in Ω and therein bounded. The $L^p(\Omega)$ is the space of p-integrable functions $(1 \leq p < \infty)$ in a domain Ω, and when $p = 2$ the $L^2(\Omega)$ inner product is denoted by $(\cdot,\cdot)_{L^2(\Omega)}$. The Hilbert space denoted by $H^m(\Omega)$ is the space of all the functions $\psi \in L^2(\Omega)$ with all the weak derivatives of order $\leq m$ that belong to $L^2(\Omega)$. The space $H_0^1(\Omega)$ consists of functions $H^1(\Omega)$ vanishing on the boundary $\partial\Omega$. The topological dual of $H_0^1(\Omega)$ is denoted by $H^{-1}(\Omega)$ and the duality pairing is denoted by $\langle\cdot,\cdot\rangle$.

With these preliminaries, the variational formulation of (1.1) reads as follows, find $u \in \mathcal{V} := H_0^1(\Omega)$ such that

$$B(u,v) = L(v) \qquad \forall v \in \mathcal{V} \tag{2.1}$$

where $B(\cdot,\cdot)$, and $L(\cdot)$ are the bilinear, and linear forms associated with the operator $\mathcal{L}$ respectively, that is,

$$B(u,v) := k(\nabla u, \nabla v)_\Omega + (\boldsymbol{a}\cdot\nabla u, v)_\Omega + s(u,v)_\Omega \tag{2.2}$$

or based on an index notation for bilinear form,

$$B(u,v) := (\partial_i v, k\partial_i u)_\Omega + (v, a_i\partial_i u)_\Omega + (v, su)_\Omega \tag{2.3}$$

and

$$L(v) := \langle f, v\rangle_\Omega \tag{2.4}$$

It is assumed that the CDR problems that have been studied in this thesis are coercive i.e. ensuring the well-posedness of the continuous problem.

Lemma 2.1 *(coercivity) for all $u \in H_0^1$, there exists a constant $M \in \mathbb{R}$ and $M > 0$ such that,*

$$B(u,u) \geq M\|u\|_{L^2}^2$$

which holds for our problem if the following conditions are assumed,

$$\begin{cases} u \quad \text{prescribed on inflows} \\ s - \frac{1}{2}\nabla \cdot a \geq 0 \\ k > 0 \end{cases} \tag{2.5}$$

proof. From definition of the bilinear form at 2.2 it follows that

$$B(u,u) = k\|\nabla u\|_{L^2}^2 + \int_\Omega \boldsymbol{a} \cdot \nabla u \, u \, d\Omega + s\|u\|_{L^2}^2 \qquad u = 0 \quad \text{on} \quad \partial\Omega \tag{2.6}$$

Using the divergence theorem, the second term of 2.6 yields as follows (based on index notation),

$$\begin{aligned} \int_\Omega a_i \partial_i \frac{u^2}{2} d\Omega \qquad &= \int_\Omega \partial_i \left(a_i \frac{u^2}{2} \right) d\Omega - \int_\Omega \partial_i a_i \frac{u^2}{2} d\Omega \\ &= \int_{\partial\Omega} a_i n_i \frac{u^2}{2} d\Gamma - \int_\Omega \partial_i a_i \frac{u^2}{2} d\Omega \end{aligned} \tag{2.7}$$

Following this and using Poincaré-Friedrich inequality it can be concluded that,

$$B(u,u) \geq \left(Ck\|u\|_{L^2}^2 \right) + \int_{\partial\Omega} \boldsymbol{a} \cdot \boldsymbol{n} \frac{u^2}{2} d\Gamma + \int_\Omega \left(s - \frac{\nabla \cdot \boldsymbol{a}}{2} \right) u^2 d\Omega \tag{2.8}$$

To hold coercivity these terms need to be positive. Hence, the following conditions must hold,

- From the first term, $k > 0$.
- From the second term, $\boldsymbol{a} \cdot \boldsymbol{n} \geq 0$. Figure 2.1 can demonstrate that this holds for the outflow boundaries, therefore u needs to be prescribed on the inflows.
- From the third term, $s - \frac{1}{2}\nabla \cdot \boldsymbol{a} \geq 0$. □

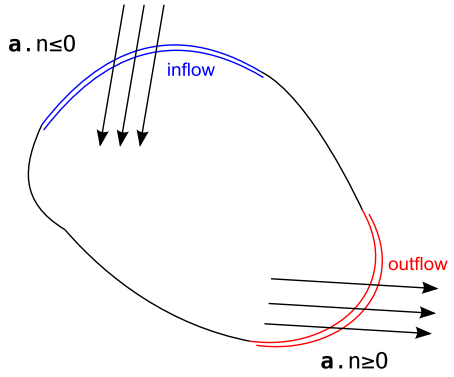

Figure 2.1: A control volume - representing inflow and outflow boundaries

Let $T_h = \{K\}$ be a finite element partition of the domain Ω into elements K, of size $h > 0$, which is assumed to be shape regular (i.e., the elements meet a minimum angle condition, uniformly with respect to h). In the continuous finite element approximation of the problem, T_h is a set of elements K which are assumed to cover Ω exactly, and are either disjoint or share a complete edge. The elements $K \in T_h$ are either triangles or quadrilaterals. Based on this partition, the space $\mathcal{V}$ have been approximated by a finite dimensional space $\mathcal{V}_h$, such that

$$\mathcal{V}_h = \left\{ v \in \mathcal{V} : v \mid_K \circ F_K^{-1} \in \mathcal{Q}_p\left(\widehat{K}\right), 1 \leq p \leq \infty \right\}$$

where $\mathcal{Q}_p\left(\widehat{K}\right)$ denotes the set of all polynomials on $\widehat{K}$ of degree p, and F is an affine mapping from the reference element $\widehat{K}$ to the physical element K, and

$$v(x) = F \circ \widehat{v}(s) \quad and \quad \widehat{v}(s) = v(x) \circ F^{-1} \tag{2.9}$$

which have been represented in figure 2.2.

Accordingly, the continuous Galerkin discrete problem yields, obtaining $u_h \in \mathcal{V}_h$ such that

$$B\left(u_h, v_h\right) = L\left(v_h\right) \qquad \forall v \in \mathcal{V}_{0,h} \tag{2.10}$$

2.2 Scale splitting and modeling of the subgrid scales

The multiscale concept originally proposed by Hughes (24) is adopted and extended to new applications. In 1998 it was shown by Hughes *et al.* (10) that stabilized methods could be derived from a variational multiscale formulation. The underlying idea of

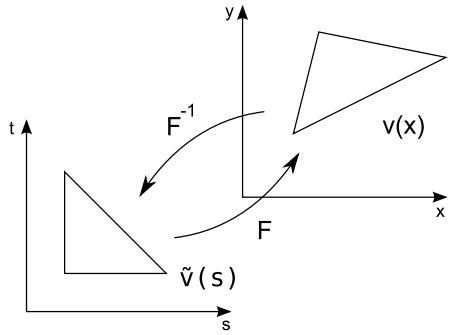

Figure 2.2: affine mapping - from reference element $\widehat{v}(s)$ to physical element $v(x)$

the VMS is based on a decomposition of the unknown u into resolvable part u_h and a subgrid scale part $\widehat{u}$ which cannot be captured by the finite element mesh, i.e.

$$u = u_h + \widehat{u} \tag{2.11}$$

which induces a decomposition of the space V as a direct sum with an appropriate projection operator as

$$V = V_h \oplus \widehat{V} \tag{2.12}$$

where $\oplus$ is a direct sum symbol, and the space $\widehat{V}$ is called the space of *subgrid scales* or *subscales*. The continuous problem is equivalent to finding $u_h \in V_h$ and $\widehat{u} \in \widehat{V}$ such that

$$B(u_h, v_h) + B(\widehat{u}, v_h) = L(v_h) \qquad \forall v_h \in V_h \tag{2.13}$$

$$B(u_h, \widehat{v}) + B(\widehat{u}, \widehat{v}) = L(\widehat{v}) \qquad \forall \widehat{v} \in \widehat{V} \tag{2.14}$$

The first equation is in the space of coarse scale V_h and consists of two terms: the first one is the Galerkin contribution and the second one takes into account the influence of the subgrid scale on the coarse scale solution u_h. The second one is an equation for the subgrid scale contribution whose effect is to be included into the first equation.

Let us simplify the notation by using the following definitions,

$$\Omega^h = \bigcup_{K \in \Omega_h} K \qquad \Gamma^h = \bigcup_{K \in \Omega_h} \partial K$$

and

$$(\cdot,\cdot)_h = \sum_{K \in \Omega_h} (\cdot,\cdot)_K, \quad (\cdot,\cdot)_{\partial h} = \sum_{K \in \Omega_h} \langle \cdot,\cdot \rangle_{\partial K}, \quad \textit{and} \quad \|\cdot\|_h^2 = \sum_{K \in \Omega_h} \|\cdot\|_K^2$$

Now using the bilinear form 2.3, some integration by parts is taken within first equation in 2.13 consisting the following terms,

$$(\partial_i v_h, k\partial_i \widehat{u})_h := -(\widehat{u}, \partial_i (k\partial_i v_h))_h + (\widehat{u}, n_i (k\partial_i v_h))_{\partial h} \tag{2.15}$$

and

$$\begin{aligned}(v_h, a_i\partial_i \widehat{u})_h &:= (v_h, \partial_i (a_i \widehat{u}))_h - (v_h, \widehat{u}\partial_i a_i)_h \\ &:= -(\widehat{u}, a_i\partial_i v_h)_h + (\widehat{u}, a_i n_i v_h)_{\partial h} - (\widehat{u}, v_h\partial_i a_i)_h \\ &:= -(\widehat{u}, \partial_i (a_i v_h))_h + (\widehat{u}, a_i n_i v_h)_{\partial h}\end{aligned} \tag{2.16}$$

In a similar way, the following integration by parts are considered for second equation 2.13,

$$(\partial_i u_h, k\partial_i \widehat{v})_h = -(\partial_i (k\partial_i u_h), \widehat{v})_h + ((kn_i)\partial_i u_h, \widehat{v})_{\partial h} \tag{2.17}$$

and

$$(\partial_i \widehat{u}, k\partial_i \widehat{v})_h = -(\partial_i (k\partial_i \widehat{u}), \widehat{v})_h + ((kn_i)\partial_i \widehat{u}, \widehat{v})_{\partial h} \tag{2.18}$$

After defining these integrations by parts, now the equations in 2.13 can be written as follows,

$$\begin{aligned} B(u_h, v_h) + (\widehat{u}, \mathcal{L}^* v_h) + (\widehat{u}, n_i (k\partial_i v_h))_{\partial h} + (\widehat{u}, a_i n_i v_h)_{\partial h} &= L(v_h) \qquad \forall v_h \in V_h \\ (\mathcal{L}\widehat{u}, \widehat{v})_h + ((kn_i)\partial_i \widehat{u}, \widehat{v})_{\partial h} + ((kn_i)\partial_i u_h, \widehat{v})_{\partial h} &= ((f - \mathcal{L}u_h), \widehat{v})_h \qquad \forall \widehat{v} \in \widehat{V}\end{aligned}$$

where $\mathcal{L}^*$ is the adjoint of the operator $\mathcal{L}$ given by

$$\mathcal{L}^*(v) = -\partial_i (k\partial_i v) - \partial_i (a_i v) + sv \tag{2.19}$$

Since these equations are for the exact problem i.e. $u = u_h + \widehat{u}$, the normal fluxes of the exact solution are continuous across the interior boundaries that is,

$$((kn_i)\partial_i u, \widehat{v})_{\partial h} = ((kn_i)\partial_i \widehat{u}, \widehat{v})_{\partial h} + ((kn_i)\partial_i u_h, \widehat{v})_{\partial h} = 0 \tag{2.20}$$

therefore the boundary terms vanish from the second equation.

Then, the second equation is equivalent to, find $\widehat{u} \in \widehat{V}$ such that

$$\begin{aligned}\mathcal{L}\widehat{u} &= R := f - \mathcal{L}u_h + \widehat{v}^{\perp} \qquad in\, \Omega^h \\ \widehat{u} &= u_{ske} \qquad on\, \Gamma^h\end{aligned} \tag{2.21}$$

where u_{ske} is a function that is defined on the element boundaries and $\widehat{v}^{\perp}$ is any function in $\widehat{V}^{\perp}$ that is the $L^2\left(\Omega^h\right)$ orthogonal complement of $\widehat{V}$. The function u_{ske} must be such that the normal fluxes of exact solution u are continuous across the element boundaries. The function $\widehat{v}^{\perp}$ is responsible to guarantee that $\widehat{u} \in \widehat{V}$, or in other words it ensures that $\mathcal{L}\widehat{u} - [f - \mathcal{L}u_h]$ belongs to $\widehat{V}^{\perp}$. It is noticed that Ω^h consists the union of the elements of the domain. Therefore any choice of u_{ske} results in n (number of elements) uncoupled equations. As in (28) the space of $\widehat{V}$ can be taken as bubble functions, that is vanishing on the element boundaries which means $u_{ske} = 0$. The choice of $u_{ske} = 0$ vanishes the boundary terms from the first equation of the subgrid scales formulation.

From the same equation 2.21 it is observed that

$$\widehat{u}|_K = \mathcal{L}^{-1}R \tag{2.22}$$

The basic idea is to approximate this equation with appropriate boundary conditions by

$$\widehat{u}|_K = \tau_K R \qquad in\, K \in \Omega_h \tag{2.23}$$

where τ_K is approximated as the inverse of the differential operator $\mathcal{L}$ on each element K. Now we need to impose the condition $\widehat{u} \in \widehat{V}$ which can be expressed as

$$\left(\widehat{u}, \widehat{\psi}^{\perp}\right) = 0 \qquad \forall \widehat{\psi}^{\perp} \in \widehat{V}^{\perp} \tag{2.24}$$

Considering an inner product weighted by τ as,

$$(\cdot, \cdot)_{\tau} = (\tau_K \cdot, \cdot) \tag{2.25}$$

and considering a projection $\widehat{P}_{\tau}^{\perp}$ onto $\widehat{V}^{\perp}$ associated to the previously defined product $(\cdot, \cdot)_{\tau}$,

$$\left(\widehat{u}, \widehat{\psi}^{\perp}\right) = \left(f - \mathcal{L}u_h, \widehat{\psi}^{\perp}\right)_{\tau} + \left(\widehat{v}^{\perp}, \widehat{\psi}^{\perp}\right)_{\tau} \qquad \forall \widehat{\psi}^{\perp} \in \widehat{V}^{\perp} \tag{2.26}$$

which implies that

$$\widehat{v}^{\perp} = -\widehat{P}_{\tau}^{\perp}\left(f - \mathcal{L}u_h\right) \tag{2.27}$$

Therefore, the expression for $\widehat{u}$ yields

$$\widehat{u} = \tau_K \widehat{P}_{\tau}\left(f - \mathcal{L}u_h\right) \tag{2.28}$$

where $\widehat{P}_{\tau} = I - \widehat{P}_{\tau}^{\perp}$ is the projection onto $\widehat{V}$ the space subscales, considering I as the identity matrix in V_h. According to (28), a typical choice of the subscales space

is $\widehat{P}_\tau = I$ which is called Algebraic SubGrid-Scale (ASGS) formulation and simply is achieved by taking $\widehat{v}^\perp = 0$ to obtain

$$\widehat{u}|_K = \tau_K \left(f - \mathcal{L}u_h\right) \tag{2.29}$$

that has been followed by this study.

Neglecting the boundary terms, the final stabilized problem yields: find $u_h \in V_h$ such that

$$B_\tau \left(u_h, v_h\right) = L_\tau \left(v_h\right) \qquad v_h \in V_h \tag{2.30}$$

where $B_\tau \left(u_h, v_h\right)$ and $L_\tau \left(v_h\right)$ are the stabilized forms, written as

$$B_\tau \left(u_h, v_h\right) = B \left(u_h, v_h\right) - \left(\mathcal{L}^* v_h, \tau \mathcal{L} u_h\right)_h \tag{2.31}$$

$$L_\tau \left(v_h\right) = L \left(v_h\right) - \left(\mathcal{L}^* v_h, \tau f\right)_h \tag{2.32}$$

2.3 Stabilized continuous finite element approximation

Having established the Variational form of CDR equation and the subgrid scales formulation by splitting the scales, in this chapter the stabilized finite element approximation of the CDR equation has been motivated. To this end, the subscale problem need to be solved and its effect be included in the coarse scale equation to derive a stabilized solution. In order to derive the approximate solution of the subscale equation, first the fine scale equation is transformed into the reference domain. This was first developed in (10) which indicates the dependence of the subgrid scale on the element size. To this end, the subscale equation has been transformed to the reference domain on each element K. Letting $\widehat{v}^\perp = 0$, we can write 2.21 as

$$\mathcal{L}\widehat{u} = r := f - \mathcal{L}u_h \tag{2.33}$$

or using the discussions in previous section and from equation 2.29,

$$\widehat{u} = \tau_K r \tag{2.34}$$

The isoparametric transformation is based on a mapping $x = F\left(\xi\right)$ from the physical element $K\left(x\right)$ to the reference element $\widehat{K}\left(\xi\right)$. Letting the following notation for the Jacobian of the corresponding transformation

$$J_{lm}^{-t} = \frac{\partial \xi_l}{\partial x_m} \tag{2.35}$$

Transformed representation of the equation (2.34) yields

$$r = J_{il}^{-t}\frac{\partial}{\partial \xi_l}\left(kJ_{im}^{-t}\frac{\partial}{\partial \xi_m}\widehat{u}\right) + a_i J_{il}^{-t}\frac{\partial}{\partial \xi_l}\widehat{u} + s\widehat{u} \qquad in\,\widehat{K} \tag{2.36}$$

Henceforth, the coefficients of CDR problem has been defined with the following notations

$$k^r = J_{il}^{-t}kJ_{im}^{-t} \tag{2.37}$$

and

$$a_i^r = a_i J_{il}^{-t} \tag{2.38}$$

and eventually the residual r in the reference domain can be written as follows,

$$r = \frac{\partial}{\partial \xi_i}\left(k^r\frac{\partial}{\partial \xi_i}\widehat{u}\right) + a_i^r\frac{\partial}{\partial \xi_i}\widehat{u} + s\widehat{u} \qquad in\,\widehat{K} \tag{2.39}$$

Fourier analysis of the subscale problem was developed by R. Codina at (28), which has been followed in the current discussion. According to this study, the resulting problem can be identified based on the Fourier representation of the Green function of the subscale equation. Following the same study, after making an approximation regarding the Green function the stabilization parameter is derived as follows,

$$\tau = \left(\left(k^r\left|\boldsymbol{\lambda}_0^2\right| + s\right)^2 + \left(\boldsymbol{a}^r\cdot\boldsymbol{\lambda}_0\right)^2\right)^{-1/2} \tag{2.40}$$

for some $\boldsymbol{\lambda}_0$, which (as it will be seen in next section) is a crucial parameter in determining an appropriate expression for τ. Eventually, after some more steps the following form of τ has been proposed in (28),

$$\tau = \left[\left(c_1k^r + s\right)^2 + \left(c_2\left|\boldsymbol{a}^r\right|\right)^2\right]^{-1/2} \tag{2.41}$$

Here according to (28), c_1 and c_2 are some constants independent of h for which equation 2.34 holds. As in the same paper, c_1 is independent of the CDR problem coefficients k, $\boldsymbol{a}$,and s, whereas c_2 only depends on the direction of the convection velocity $\boldsymbol{a}$ but not its magnitude. Moreover, the constant c_1 can be identified with $|\boldsymbol{\lambda}_0|^2$ and c_2 with $|\boldsymbol{\lambda}_0|\,|cos\alpha|$, where α is the angle between $\boldsymbol{a}$ and $\boldsymbol{\lambda}_0$. Since $\boldsymbol{\lambda}_0$ depends on the residual r in equation 2.33, consequently the constants c_1 and c_2 will also depend on that. Hence, ascertaining the value of $\boldsymbol{\lambda_0}$ seems to be a key issue in formulating stabilized finite element using VMS.

2.3.1 Calculation of the stabilization parameter

Having derived the functional form of the stabilization parameters, in this part the demand is to establish a value for $\boldsymbol{\lambda}_0$ which from now on will be denoted without its superscript for simplicity.

A 1D case. Firstly, a one dimensional case has been considered. The CDR coefficients appearing in the stabilization parameter has been replaced by their values in a reference domain defined within $[-1, 1]$, with a length defined by $h_{nat} = 2$, and it is considered that for any order of approximation the elements are such that the mapping from reference element $K(\xi)$ to physical element $K(x)$ is linear, that is, for an element in domain x with $e_x \in [a, b]$ and a length h, a linear mapping defined as follows

$$\xi = \frac{h_{nat}}{h} x - \frac{h_{nat}}{2} \frac{a+b}{h} \tag{2.42}$$

transforms the element e_ξ from reference domain ξ ($e_\xi \in [-1, 1]$) to the physical domain x. Hence, the Jacobian of the transformation is constant and we have

$$J_{ij}^{-t} = \frac{h_{nat}}{h} \tag{2.43}$$

Hence, the stabilization parameter holds

$$\tau = \left[\left(\frac{k h_{nat}^2 \lambda^2}{h^2} \right)^2 + \left(\frac{h_{nat} \lambda a}{h} \right)^2 \right]^{-1/2} \tag{2.44}$$

According to (29), an optimal choice for λ (in one dimensional case) that guarantees exact nodal values would be

$$\lambda = \frac{2}{h_{nat}} \tag{2.45}$$

and the final expression for the stabilization parameter in one dimensional case yields

$$\tau = \left[\left(\frac{4k}{h^2} \right)^2 + \left(\frac{2a}{h} \right)^2 \right]^{-1/2} \tag{2.46}$$

It is observed that the final expression for the stabilization parameter does not depend on the reference domain. According to R. Codina *et al.* (31), obtaining exact nodal values in the case of quadratic elements is not feasible and they have offered the following value as an optimal choice,

$$\lambda = \frac{4}{h_{nat}} \tag{2.47}$$

A General 2D case. Considering a case with constant convection velocity and assuming that the problem is such that one direction of the reference domain coincides with the streamlines, the problem can be regarded as one dimensional in this direction and a pure diffusion problem in the orthogonal directions. As in (30), this implies that the diffusion needed to define the Peclet number is the one along the streamlines, what suggest to take $\boldsymbol{\lambda} = \frac{\boldsymbol{a}^r}{\|\boldsymbol{a}^r\|}$, using this and from 2.40 we have

$$\tau = \left[\left(\frac{a_i^r a_j^r}{\|\boldsymbol{a}^r\|^2} k^r + s \right)^2 + \|\boldsymbol{a}^r\|^2 \right]^{-1/2} \tag{2.48}$$

Now, considering a constant convection velocity $\boldsymbol{a} = (a_1, a_2)$ in a two dimensional CDR problem with reference element side lengths of h_1, and h_2 in streamline direction and perpendicular one respectively we have,

$$\boldsymbol{a}^r = a_i J_{il} = \left(\frac{2a_1}{h_1}, \frac{2a_2}{h_2} \right)^t \tag{2.49}$$

Hence, from 2.48 the expression for τ gives

$$\tau = \left[\left(\frac{4k}{h_k^2} \right)^2 + \left(\frac{2\|\boldsymbol{a}\|}{h_a} \right)^2 \right]^{-1/2} \tag{2.50}$$

where

$$h_k^2 = \frac{1}{4}\|\boldsymbol{a}^r\|^2 \left(\frac{a_1^2}{h_1^4} + \frac{a_2^2}{h_2^4} \right)^{-1} \tag{2.51}$$

$$= \left[\frac{a_1^2}{h_1^2} + \frac{a_2^2}{h_2^2} \right] \left(\frac{a_1^2}{h_1^4} + \frac{a_2^2}{h_2^4} \right)^{-1} \tag{2.52}$$

and

$$h_a = 2\frac{\|\boldsymbol{a}\|}{\|\boldsymbol{a}^r\|} \tag{2.53}$$

are the length scales which are dependent on the velocity direction. It is noticed that this formula is valid for first order approximations, and in order to extend it to higher order approximations the effect of polynomial degree p must be included which can be better explained through the following case.

2D case with one dimensional convection velocity. For a one dimensional convection velocity of the form $\boldsymbol{a} = (a, 0)^t$, including the effect of polynomial approximations and using 2.50 the expression for τ gives, using

$$\begin{aligned} \tau &= \left[\left(\frac{4k}{\left(\frac{h_1}{p}\right)^2} \right)^2 + \left(\frac{2a}{\left(\frac{h_1}{p}\right)} \right)^2 \right]^{-1/2} \\ &\approx \left[\frac{4k}{\left(\frac{h_1}{p}\right)^2} + \frac{2a}{\left(\frac{h_1}{p}\right)} \right]^{-1} \end{aligned} \tag{2.54}$$

where $\frac{h_1}{p}$ is the distance between each two nodes. This expression implies that refinement of the mesh only in the direction of $\boldsymbol{a}$ makes sense, and any refinement in the direction orthogonal to $\boldsymbol{a}$ will not affect the solution. Roughly speaking, refining the mesh in this case is like adding diffusion (looking into $\frac{4k}{\left(\frac{h_1}{p}\right)^2}$ factor). Furthermore since the refinement behaves like adding diffusion in only one direction, the added diffusion is anisotropic. In some references such as in (36) for quadratic elements, and also in (35), the effect of the polynomial approximations has been included in the diffusion term of the stabilization parameter, that is,

$$\tau \approx \left[\frac{4k}{\left(\frac{h_1}{p^2}\right)^2} + \frac{2a}{\left(\frac{h_1}{p}\right)} \right]^{-1} \tag{2.55}$$

where the term $\frac{4k}{\left(\frac{h_1}{p}\right)^2}$ in 2.54 has been replaced by $\frac{4k}{\left(\frac{h_1}{p^2}\right)^2}$ by increasing the total power of polynomial approximation from p^2 to p^4 in diffusion term. In our calculations we have implemented 2.55.

3

Discontinuous Galerkin approximation

The discontinuous Galerkin (DG) finite element methods are popularly emerging for the numerical solution to partial differential equations. The first DG method was introduced in 1973 by Reed and Hill (32) for solving hyperbolic equations of the steady-state neutron transport. since then, there has been an active development of DG methods for hyperbolic and nearly hyperbolic problems. Several schemes have been proposed for the discretization of the viscous terms. Among the various alternatives some of them include, the method proposed by Bassi and Rebay (1) for the compressible Navier-Stokes equations, or Local Discontinuous Galerkin (LDG) method introduced by Cockburn and Shu (27) for Convection-Diffusion problems, and a Compact Discontinuous Galerkin (CDG) method introduced by Peraire and Persson in (33). Also, the Interior Penalty (IP) methods originally introduced by Douglas and Dupont in (26) in 1970, were developed for discretization of elliptic and parabolic equations using discontinuous finite elements. The development of the IP methods was independent from the development of DG methods for hyperbolic equations. A unified analysis of the various DG methods dealing with elliptic problems was proposed by Arnold *et al.* can be found in (9). DG methods offer several advantages such as, in design of higher order approximations due to the fact that elements of varying order of accuracy can be selected for the same mesh which allows for *hp*-adaptive refinement, built-in stability, rather easy implementation on unstructured meshes with hanging nodes, being locally conservative, locality of the method where the discontinuities occur only on element edges/faces, and

being more efficient for parallelization. Despite the attractive features of DG methods, there are also some shortcomings that limit their practical utility. Foremost among is the size of DG linear system as a result of node duplication on edges/faces and obviously increasing the costs. The attractive features of DG methods, have already suited them for variety of applications such as in aeroacoustic, turbomachinery, gas dynamics, turbulent flows, electro-magnetism, semiconductor device simulation, and Granular materials among many other applications that for more information can be referred to (7).

3.1 Hybrid form of the problem

In this section, Discontinuous Galerkin approximation has been derived from a hybrid form of the problem. The strong form of CDR equation including the Neumann boundary conditions have been shown in the following,

$$\begin{aligned} &\mathcal{L}u := -k\Delta u + \boldsymbol{a}\cdot\nabla u + su = f \qquad && in\,\Omega, \\ &u = 0 && on\,\Gamma_D, \\ &\mathcal{T}(u) := k\partial_n u = q && on\,\Gamma_N. \end{aligned} \tag{3.1}$$

where $\Omega \subset \mathbb{R}^d$ is a bounded domain with boundary $\partial\Omega := \Gamma = \Gamma_D \cup \Gamma_N$, considering Γ_D and Γ_N as the Dirichlet and Neumann boundaries respectively.

Then the variational form of 3.1 yields, find $u \in V := H_0^1(\Omega)$ such that

$$B(u,v) = L(v) \qquad \forall v \in V \tag{3.2}$$

where

$$B(u,v) := k(\nabla u, \nabla v)_\Omega + (\boldsymbol{a}\cdot\nabla u, v)_\Omega + s(u,v)_\Omega \tag{3.3}$$

and

$$L(v) := \langle f, v\rangle_\Omega + \langle q, v\rangle_{\partial\Omega_N} \tag{3.4}$$

Now let us rewrite the bilinear form 3.2 as,

$$B(u,v) = (\mathcal{L}(u), v)_\Omega + \langle \mathcal{T}(u), v\rangle_{\partial\Omega} \tag{3.5}$$

then by taking use of the following operators

$$\mathcal{L}^* := -k\Delta v - \nabla \cdot (\boldsymbol{a}v) + sv, \tag{3.6}$$

$$\mathcal{T}^* := k\partial_n v + \boldsymbol{n} \cdot \boldsymbol{a}v \tag{3.7}$$

and taking integral by parts we have that,

$$\begin{aligned} B(u,v) &= \\ &= -(ku, \nabla v) + \langle ku, \nabla v \cdot \boldsymbol{n}\rangle_{\partial\Omega} - (u, \boldsymbol{a} \cdot \nabla v) && (3.8) \\ &+ \langle u, v\boldsymbol{a} \cdot \boldsymbol{n}\rangle_{\partial\Omega} - (u, v\nabla \cdot \boldsymbol{a}) + s(u,v) \\ &= -(u, k\nabla v - \nabla \cdot (\boldsymbol{a}v) + sv) + \langle u, k\nabla v \cdot \boldsymbol{n} + v\boldsymbol{a} \cdot \boldsymbol{n}\rangle_{\partial\Omega} \\ &= (u, \mathcal{L}^*(v)) + \langle u, \mathcal{T}^*(v)\rangle_{\partial\Omega} && (3.9) \end{aligned}$$

Let $T_h = \{K\}$ be a finite element partition of the domain Ω into elements K, of size $h > 0$, which is assumed to be shape regular (i.e., the elements meet a minimum angle condition, uniformly with respect to h). In the DG finite element approximation of the problem, T_h is a set of non-conforming elements K with disjoint interior boundaries that may possess hanging nodes. The elements $K \in T_h$ are either triangular or quadrilateral. It has been considered that the elements cover Ω exactly or Ω is a polyhedron. For a generic element K in T_h, we denote h_K as the diameter of K and n_K as its outward unit normal. Let $\mathcal{E}_h$ be the set of elemental edges consisting with, $\mathcal{E}_h^i$ the set of all internal edges, and $\mathcal{E}_h^{\partial\Omega}$ the set of boundary edges, following

$$\mathcal{E}_h = \mathcal{E}_h^i \cup \mathcal{E}_h^{\partial\Omega}. \tag{3.10}$$

For an interior edge F of the mesh, let us assume that there are $K^-(F)$ and $K^+(F)$ in T_h sharing this edge such that $F = K^-(F) \cap K^+(F)$ then we define,

$$K^-(F) = \{K(F) \in T_h | \boldsymbol{a} \cdot n_K > 0\} \tag{3.11}$$

and

$$K^+(F) = \{K(F) \in T_h | \boldsymbol{a} \cdot n_K \leq 0\} \tag{3.12}$$

which can be checked through a sample case shown in figure 3.1. In order to formulate a DG discretization, it is needed to define jumps $[\![\cdot]\!]$ and averages $\{\cdot\}$ on $\mathcal{E}_h$. Let us consider two elements K^- and K^+ sharing the edge, and n^- and n^+ being their

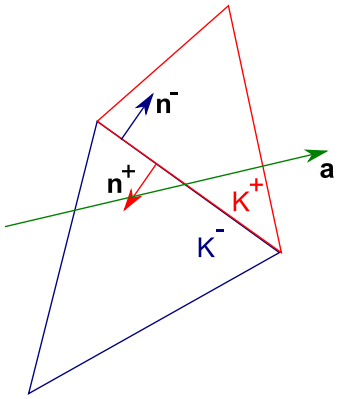

Figure 3.1: Discontinuous Elements - Schematic view of normals and elements sharing an edge

outward normals as shown in figure 3.1. Accordingly, for a given scalar field ϕ over an edge/face $e \in \mathcal{E}_h^i$ we define,

$$\begin{aligned}\llbracket \boldsymbol{n}\phi \rrbracket &:= \boldsymbol{\phi}^- \boldsymbol{n}^- + \boldsymbol{\phi}^+ \boldsymbol{n}^+, \\ \{\boldsymbol{n}\phi\} &:= \frac{1}{2}\left(\boldsymbol{\phi}^- \boldsymbol{n}^- + \boldsymbol{\phi}^+ \boldsymbol{n}^+\right).\end{aligned}$$

It is noticed that in DG discretization of the problem, the finite element space will not lie on $H^1(\Omega)$ (as in the continuous case) because it will consist of discontinuous elements, but rather it will be in the piecewise Sobolev space, denoted by $H^1_{ps}(K)$ and defined as

$$H^1_{ps}(K) = \left\{ v \in L^2(\Omega) \,\middle|\, v|_K \in H^1(K) \,\forall K \in T_h \right\} \tag{3.13}$$

Following this, the broken space V has been defined as $V := H^1_{ps}(K)$, which particularly denotes the spaces of functions whose restriction to each element K belongs to the Sobolev space $H^1(K)$. Furthermore, the finite element subspaces $V_h \subset V$ have been defined as follows

$$V_h = \left\{ v \in V : v\,|_K \circ F_K^{-1} \in \mathcal{Q}_p\left(\widehat{K}\right), 1 \leq p \leq \infty \right\}$$

where $\mathcal{Q}_p\left(\widehat{K}\right)$ denotes the set of all polynomials on $\widehat{K}$ of degree p, and F is an affine mapping from the reference element $\widehat{K}$ to the physical element K.

The idea is to use a three-field hybrid formulation, taking as unknowns, the main field in the interior elements u_h, and its fluxes λ_h and traces γ_h on the element boundaries. Also a closed form expression have been proposed for the fluxes and traces based

on, finite difference expressions to compute the fluxes in terms of the element unknown and its traces, and imposition of flux continuity for computing the traces.

The abstract variational problem within each element would be, find $u_h \in V_h$ such that

$$B\left(u_h, v_h\right) = L\left(v_h\right) \qquad \forall v_h \in V_h \tag{3.14}$$

In order to formulate the hybrid problem it is required to weakly impose the boundary conditions. To this end, the boundary conditions over the sharing face can be considered as

$$\begin{cases} u_1 = \gamma \\ u_2 = \gamma \end{cases} \qquad \forall \gamma \in E \tag{3.15}$$

and

$$\lambda_1 = \lambda_2 \quad or \quad k_1 n_1 \cdot \nabla u_1 = k_2 n_2 \cdot \nabla u_2 \qquad \forall \lambda \in F \tag{3.16}$$

where E, and F are the spaces which have been defined as follows,

$$F = \left\{ \mu : \bigcup K \to \mathbb{R} \middle| v|_K \in \mathcal{Q}_{Pf}\left(\partial K\right), K \in \mathcal{Q}_h \right\},$$
$$E = \left\{ \kappa : \bigcup e \to \mathbb{R}\big|_e \in \mathcal{Q}_{Pe}\left(e\right), e \in \mathcal{E}_h, \, and \, \kappa|_e = 0 \, if \, e \subset \gamma_D \right\}$$

Using equation 3.2, if we write the bilinear form for each element then we have, find $u_h \in V_h$ such that

$$B\left(u_h, v_h\right) - \left\langle \lambda, v_h \right\rangle_{\partial K} = L\left(v_h\right) \qquad \forall v_h \in V_h \quad and \quad \forall \lambda \in F \tag{3.17}$$

Henceforth, weakly imposing the boundary conditions on each element we can write

$$\left\langle \mu, u_h - \gamma \right\rangle_{\partial K} = 0 \qquad \forall \mu \in F, \tag{3.18}$$

$$\left\langle \kappa, \lambda \right\rangle_{\partial K} = 0 \qquad \forall \kappa \in E \tag{3.19}$$

let us consider two neighbor elements K_1, and K_2 from partition T_h of domain Ω (figure 3.1). It is noticed that over the sharing face, the conditions $u_1 = u_2$ and $\lambda_1 = \lambda_2$ must hold for the solution and the fluxes respectively.

Then the hybrid formulation for these elements reads as follows, find $u_i \in V_{hi}$, $\lambda_i \in \digamma_i\,(i=1,2)$, and $\gamma \in E$ such that

$$B_1(u_1,v_1) - \langle \lambda_1, v_1\rangle_{\partial K} = L_1(v_1) \qquad \forall v_1 \in V_{h1} \tag{3.20}$$

$$B_2(u_2,v_2) - \langle \lambda_2, v_2\rangle_{\partial K} = L_2(v_2) \qquad \forall v_2 \in V_{h2} \tag{3.21}$$

$$\langle \mu_1, u_1 - \gamma\rangle_{\partial K} = 0 \qquad \forall \mu_1 \in \digamma_1, \tag{3.22}$$

$$\langle \mu_2, u_2 - \gamma\rangle_{\partial K} = 0 \qquad \forall \mu_2 \in \digamma_2, \tag{3.23}$$

$$\langle \kappa, \lambda_1 + \lambda_2\rangle_{\partial K} = 0 \qquad \forall \kappa \in E \tag{3.24}$$

Introducing the notations,

$$\Omega^h = \underset{K\in\Omega_h}{\cup} K, \qquad \Gamma^h = \underset{K\in\Omega_h}{\cup} \partial K$$

and

$$B_h(\cdot,\cdot) = \sum_{K\in\Omega_h} B_K(\cdot,\cdot), \quad L_h(\cdot,\cdot) = \sum_{K\in\Omega_h} L_K(\cdot,\cdot), \quad (\cdot,\cdot)_h = \sum_{K\in\Omega_h} (\cdot,\cdot)_K,$$
$$(\cdot,\cdot)_{\partial h} = \sum_{K\in\Omega_h} \langle\cdot,\cdot\rangle_{\partial K}, \quad \textit{and} \quad \|\cdot\|_h^2 = \sum_{K\in\Omega_h} \|\cdot\|_K^2$$

then the following expression can be written for the hybrid problem over the whole domain,

find $u_h \in V_h$, $\lambda \in \digamma$, and $\gamma \in E$ such that

$$\begin{aligned} &B_h(u_h,v_h) - (\lambda, v_h)_{\partial h} = L_h(v_h) \qquad \forall v_h \in V_h \\ &(\mu, u_h - \gamma)_{\partial h} = 0 \qquad \forall \mu \in \digamma, \\ &(\kappa, \lambda)_{\partial h} = 0 \qquad \forall \kappa \in E \end{aligned} \tag{3.25}$$

where u_h is the approximate solution.

3.2 Approximation of the fluxes and the traces

In the previous section a three field hybrid problem was derived (3.25). In order to solve the proposed problem, the equations for fluxes and traces need to be approximated numerically. The key point to step to the proposed method is to design expressions for computing the fluxes λ and the traces γ from finite difference-like approximations. The steps that have been proposed can be listed as:

1. Computing the fluxes λ based on values of u_h, γ using finite difference-like expressions.

2. Computing the traces γ by imposing continuity of total fluxes.

3. substituting the values of γ obtained in step. 2, in expression of λ derived at step. 1, to achieve an expression for λ only in terms of the unknowns u_h.

Approximation of fluxes. A schematic view of discontinuous neighboring elements has been illustrated by figure 3.2.

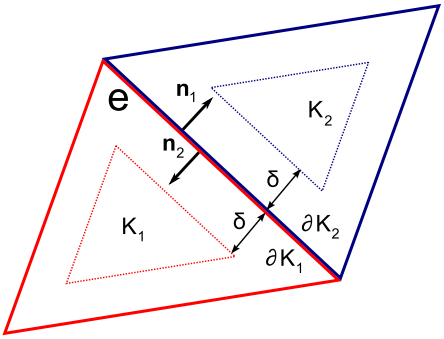

Figure 3.2: Neighboring discontinuous elements - A schematic view representing the distance δ

Let us assume that the approximation u_h is meaningful to compute the fluxes λ up to a distance δ from the edge e (as shown in figure 3.2), on which the trace takes a value γ. Then the distance δ will be a parameter of the formulation. Using a finite difference-like approach the fluxes can be approximated as

$$\lambda^{\pm} \approx \frac{k^{\pm}}{\delta}\left(\gamma - u_{h_\delta}^{\pm}\right)$$

where $u_{h_\delta}^{\pm}$ can be approximated as

$$u_{h_\delta}^{\pm} = u_h^{\pm} - \delta\partial_{n^{\pm}} u_h^{\pm} + \mathcal{O}\left(\delta^2\right),$$

which gives,

$$\lambda^{\pm} \approx \frac{k^{\pm}}{\delta}\left(\gamma - u_h^{\pm}\right) + k^{\pm}\partial_{n^{\pm}} u_h^{\pm} \tag{3.26}$$

In figure 3.3, the idea for approximation of the fluxes between two neighboring elements has been visualized.

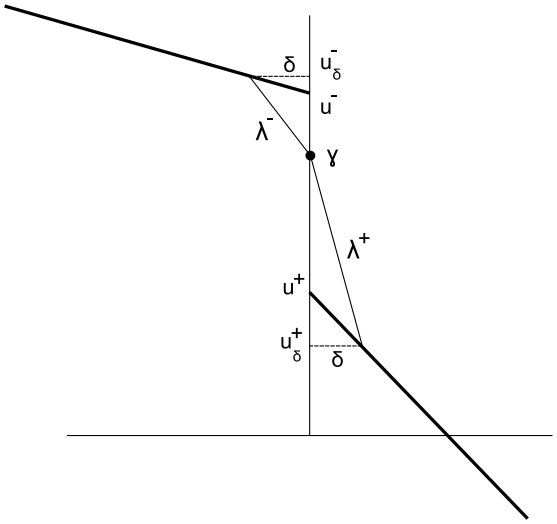

Figure 3.3: Approximation of the fluxes for two neighboring elements

Approximation of traces. The second step consists of imposing continuity of total fluxes i.e. the diffusive fluxes $k\partial_n u$ and convective fluxes $\boldsymbol{n}\cdot\boldsymbol{a}u$. Then for neighboring discontinuous elements K_1 and K_2 sharing an edge $e \in \mathcal{E}_h^i$, with diffusion coefficients k_1 and k_2, the continuity of the total fluxes for an approximation solution $u_h \in V_h$ yields,

$$\begin{aligned} 0 &= [\![\mathcal{T}(u)]\!] + [\![\boldsymbol{n}\cdot\boldsymbol{a}u]\!] \\ &\approx (\lambda_1 + \lambda_2) + [\![\boldsymbol{n}\cdot\boldsymbol{a}u_h]\!] \\ &\approx \frac{1}{\delta}\left[(k_1+k_2)\,\gamma - k_1 u_{h1} - k_2 u_{h2}\right] + [\![\mathcal{T}(u_h) + \boldsymbol{n}\cdot\boldsymbol{a}u_h]\!] \\ &\approx [\![\mathcal{T}(u_h) + \boldsymbol{n}\cdot\boldsymbol{a}u_h]\!] + \frac{2}{\delta}\left(\{k\}\,\gamma - \{ku_h\}\right). \end{aligned}$$

Hence, an expression for γ can be derived as

$$\gamma = \frac{\{ku_h\}}{\{k\}} - \frac{\delta}{2\,\{k\}}[\![\mathcal{T}(u_h) + \boldsymbol{n}\cdot\boldsymbol{a}u_h]\!]. \tag{3.27}$$

Final expression of the fluxes. Using the expressions derived in last two steps, an expression have been derived for fluxes λ in terms of u_h by replacing the derived expression of γ in λ, that is,

$$\begin{aligned} \lambda &= \frac{k}{\delta}(\gamma - u_h) + \mathcal{T}(u_h) \\ &= \frac{k}{\delta}\left(\frac{\{ku_h\}}{\{k\}} - u_h\right) - \frac{k}{2\,\{k\}}[\![\mathcal{T}(u_h) + \boldsymbol{n}\cdot\boldsymbol{a}u_h]\!] + \mathcal{T}(u_h). \end{aligned} \tag{3.28}$$

Let us consider a harmonic average $\langle\cdot\rangle$ for diffusion coefficient defined as

$$\langle k\rangle := \frac{k_1 k_2}{\{k\}} = \frac{2k_1 k_2}{k_1 + k_2} \tag{3.29}$$

between two neighboring elements. Now defining $\{\mathcal{T}(u_h)\} = \langle k\rangle \boldsymbol{n}\cdot\{\nabla u_h\}$, finally we obtain,

$$\lambda = -\frac{\langle k\rangle}{2\delta}\boldsymbol{n}\cdot[\![\boldsymbol{n}u_h]\!] + \{\mathcal{T}(u_h)\} - \frac{k}{2\{k\}}[\![\boldsymbol{n}\cdot\boldsymbol{a}u_h]\!]. \tag{3.30}$$

Fluxes, traces and their test functions. Based on the traces and fluxes obtained in 3.27 and 3.30 respectively, the test functions may be taken as,

$$\kappa = \frac{\{kv\}}{\{k\}} - \frac{\delta}{2\{k\}}[\![\mathcal{T}^*(v) - \boldsymbol{n}\cdot\boldsymbol{a}v]\!], \tag{3.31}$$

for fluxes, and

$$\mu = -\frac{\langle k\rangle}{2\delta}\boldsymbol{n}\cdot[\![\boldsymbol{n}v]\!] + \{\mathcal{T}^*(v)\} - \frac{k}{2\{k\}}[\![\boldsymbol{n}\cdot\boldsymbol{a}v]\!]. \tag{3.32}$$

for traces, with $v \in V_h$.

Resulting DG approximation, constant k. Considering a constant diffusion coefficient k over the domain, the general expressions obtained for traces, fluxes, and their corresponding test functions yield,

$$\gamma = \{u_h\} - \frac{\delta}{2k}[\![\mathcal{T}(u_h) + \boldsymbol{n}\cdot\boldsymbol{a}u_h]\!], \tag{3.33}$$

$$\lambda = -\frac{k}{2\delta}\boldsymbol{n}\cdot[\![\boldsymbol{n}u_h]\!] + \{\mathcal{T}(u_h)\} - \frac{1}{2}[\![\boldsymbol{n}\cdot\boldsymbol{a}u_h]\!], \tag{3.34}$$

$$\tag{3.35}$$

and noting the definition for $\mathcal{T}^*(v)$ introduced at 3.6, we have,

$$\begin{aligned}\kappa &= \{v\} - \frac{\delta}{2k}[\![\mathcal{T}(v) + \boldsymbol{n}\cdot\boldsymbol{a}v - \boldsymbol{n}\cdot\boldsymbol{a}v]\!] \\ &= \{v\} - \frac{\delta}{2k}[\![\mathcal{T}(v)]\!]\end{aligned} \tag{3.36}$$

and

$$\mu = -\frac{k}{2\delta}\boldsymbol{n}\cdot[\![\boldsymbol{n}v]\!] + \{\mathcal{T}(v)\}. \tag{3.37}$$

The original equation is,

$$B_h(u_h, v) - (\lambda, v)_{\partial h} + (\lambda, \kappa)_{\partial h} + (\gamma - u, \mu)_{\partial h} = L_h(v) \tag{3.38}$$

after replacing the obtained values of fluxes and traces, the following expression yields,

$$\begin{aligned}
&B_h\left(u_h, v_h\right) \\
&-\left(-\frac{k}{2\delta}\boldsymbol{n}\cdot[\![\boldsymbol{n}u_h]\!]+\{\mathcal{T}\left(u\right)\}-\frac{1}{2}[\![\boldsymbol{n}\cdot\boldsymbol{a}u_h]\!], v_h\right)_{\partial h}+ \\
&\left(-\frac{k}{2\delta}\boldsymbol{n}\cdot[\![\boldsymbol{n}u_h]\!]+\{\mathcal{T}\left(u\right)\}-\frac{1}{2}[\![\boldsymbol{n}\cdot\boldsymbol{a}u_h]\!], \{v_h\}-\frac{\delta}{2k}[\![\mathcal{T}\left(v_h\right)]\!]\right)_{\partial h} \\
&+\left(\{u_h\}-\frac{\delta}{2k}[\![\mathcal{T}\left(u_h\right)+\boldsymbol{n}\cdot\boldsymbol{a}u_h]\!]-u_h, -\frac{k}{2\delta}\boldsymbol{n}\cdot[\![\boldsymbol{n}v_h]\!]+\{\mathcal{T}\left(v_h\right)\}\right)_{\partial h} \\
&=L_h\left(v_h\right)
\end{aligned} \tag{3.39}$$

Let us add the following definition,

$$\left(\cdot,\cdot\right)_{\mathcal{E}}=\sum_{E}\left\langle\cdot,\cdot\right\rangle_{E}$$

over the element edges. Thus, writing the above equation in a more compact form the final expression for the proposed DG formulation reads,

$$\begin{aligned}
&B_h\left(u_h, v_h\right)+\frac{k}{\delta}\left([\![\boldsymbol{n}u_h]\!], [\![\boldsymbol{n}v_h]\!]\right)_{\mathcal{E}}+\frac{\delta}{2}\left([\![\boldsymbol{n}\cdot\nabla v_h]\!], [\![\boldsymbol{n}\cdot\boldsymbol{a}u_h]\!]\right)_{\mathcal{E}} \\
&-\left([\![\boldsymbol{n}u_h]\!], k\left\{\nabla v_h\right\}\right)_{\mathcal{E}}-\left([\![\boldsymbol{n}v_h]\!], k\left\{\nabla u_h\right\}\right)_{\mathcal{E}}=L_h\left(v_h\right)
\end{aligned} \tag{3.40}$$

In the obtained formulation, the interior penalty method has been recovered, adjoint consistency is ensured and also there is a built-in convective flux continuity $\frac{\delta}{2}\left([\![\boldsymbol{n}\cdot\nabla v_h]\!], [\![\boldsymbol{n}\cdot\boldsymbol{a}u_h]\!]\right)_{\mathcal{E}}$ whose effect is similar (the same in 1-D) as the more common $\frac{\delta}{2}\left(\{v_h\}, [\![\boldsymbol{n}\cdot\boldsymbol{a}u_h]\!]\right)_{\mathcal{E}}$ flux continuity (that can be seen for example in (34)).

The treatment of the discontinuous part through a hybrid formulation has introduced some features that are non-standard in discontinuous Galerkin methods, in particular,

- Compared to most of the DG formulations which are usually derived by ad-hoc approaches, in the DG method obtained here all the terms are derived in a sense naturally.

- Harmonic averages rather than arithmetic averages of discontinuous coefficients have been justified.

- It is possible to devise extensions by proposing ways to compute the fluxes other than what have been used in the current formulation

– convective flux continuity arises naturally

– Though it is very convenient to introduce additional stabilization

3.3 Stabilized discontinuous finite element approximation

Discontinuous Galerkin (DG) methods offer several important computational advantages over their continuous Galerkin counterparts (3) as it was discussed at the beginning of the current chapter. There has been recent interest in applying DG to elliptic problems for modeling of advective-diffusive problems (4, 5, 6). High-order DG methods have been the center of many studies to deal with nonlinear conservation laws and convection-dominated problems in CDR problems. Different methods have been proposed for DG discretization of elliptic problems such as BR2 (1), IP (26), LDG (27) and so on. A unified analysis of DG methods proposed by Arnold *(*et al). in (9) show the importance of consistency and stability terms in design of the DG methods. They suggest that the stabilization of DG methods via the inclusion of a penalty term is crucial, such that without it convergence is degraded or lost. Penalizing the jumps across neighboring elements by introduction of penalty terms is a typical stabilizing procedure in the context of DG finite elements. Due to existence of built-in stability terms, DG methods are felt to have advantages of robustness over conventional Galerkin methods. However, it seems that the vaunted robustness of the DG method has been to some extent overstated (specially for low order DG methods). For instance, simple one-dimensional examples of pure advection and pure diffusion were shown to give rise to spurious oscillations in Hughes *et al.* (2). Hence, further considerations for stabilization of DG methods, especially in elliptic problems such as convection-dominated ones in CDR equations, seem to be essential.

The word 'stabilization' identifies all the terms in DG formulation which enforce its stability properties. A study by Brezzi et al. (8) show that the use of jump penalties, upwinding and HughesFranca-type residual-based stabilizations (variational multiscale methods) are all different forms of the same mechanism. Thus to achieve good convergence characteristics and stable results, the key mechanism is the use of stabilization terms, which in some sense penalize the continuity constraints such that, when overpenalizing, the solution behaves close to continuous space (but of course not exactly the same).

The method proposed in this study for stabilization of the DG discretized CDR problem is through the variational multiscale (VMS) methods. An introduction to VMS method was proposed in Chapter. 2 and was developed for CDR problem in the space of conforming elements. A simultaneous approach will be followed here for DG problem resulting in a stabilized DG solution.

Following the procedure explained in Chapter. 2, here also we start by decomposition of the unknown u into resolvable part u_h and a subgrid scale unresolved part $\widehat{u}$, that is,

$$u = u_h + \widehat{u} \tag{3.41}$$

which induces a decomposition of the broken space V into the coarse and fine scale spaces V_h, and $\widehat{V}$ respectively by a direct sum i.e. $V = V_h \oplus \widehat{V}$. Then the discontinuous problem yields, finding $u_h \in V_h$, and $\widehat{u} \in \widehat{V}$ such that,

$$B\left(u_h, v_h\right) + B\left(\widehat{u}, v_h\right) = L\left(v_h\right) \qquad \forall v_h \in V_h \tag{3.42}$$

$$B\left(u_h, \widehat{v}\right) + B\left(\widehat{u}, \widehat{v}\right) = L\left(\widehat{v}\right) \qquad \forall \widehat{v} \in \widehat{V} \tag{3.43}$$

Let us express the DG formulation derived in the previous section by writing the terms associated with the boundaries denoted by $\mathcal{E}\left(u, v\right)$ of the elements as, find $u_h \in V_h$ such that

$$B_h\left(u_h, v_h\right) + \mathcal{E}\left(u_h, v_h\right) = L_h\left(v_h\right) \tag{3.44}$$

Then following the same steps introduced in Chapter (2.2), the VMS formulation of the DG problem can be expressed as follows

$$\begin{aligned}
B_h\left(u_h, v_h\right) &+ \left(\widehat{u}, \mathcal{L}^* v_h\right) + \left(\widehat{u}, n_i\left(k\partial_i v_h\right)\right)_{\partial h} \\
&+ \left(\widehat{u}, a_i n_i v_h\right)_{\partial h} + \mathcal{E}\left(u_h, v_h\right) + \mathcal{E}\left(\widehat{u}, v_h\right) = L\left(v_h\right) \qquad \forall v_h \in V_h, \\
\left(\mathcal{L}\widehat{u}, \widehat{v}\right)_h &+ \left(\left(kn_i\right)\partial_i \widehat{u}, \widehat{v}\right)_{\partial h} + \left(\left(kn_i\right)\partial_i u_h, \widehat{v}\right)_{\partial h} \\
&+ \mathcal{E}\left(u_h, \widehat{v}\right) + \mathcal{E}\left(\widehat{u}, \widehat{v}\right) = \left(\left(f - \mathcal{L}u_h\right), \widehat{v}\right)_h \qquad \forall \widehat{v} \in \widehat{V}
\end{aligned}$$

where $\mathcal{L}^*$ is the same adjoint operator defined previously. Approximating the subscales equation by considering $\widehat{u}$ as bubble function (vanishing over element boundaries), the

boundary terms will be removed unless the one including the general ingredients of the DG boundary terms in the first equation, that is,

$$\begin{aligned} &B_h\left(u_h, v_h\right) + \left(\widehat{u}, \mathcal{L}^* v_h\right)_h + \mathcal{E}\left(u_h, v_h\right) = L\left(v_h\right) \quad \forall v_h \in V_h \\ &\left(\mathcal{L}\widehat{u}, \widehat{v}\right)_h = \left(\left(f - \mathcal{L}u_h\right), \widehat{v}\right)_h \qquad\qquad \forall \widehat{v} \in \widehat{V} \end{aligned} \tag{3.45}$$

Simplifying the second equation gives, find $\widehat{u} \in \widehat{V}$ such that,

$$\begin{aligned} \mathcal{L}\widehat{u} &= R := f - \mathcal{L}u_h + \widehat{v}^{\perp} \qquad in\, \Omega^h \\ \widehat{u} &= u_{ske} \qquad on\, \Gamma^h \end{aligned} \tag{3.46}$$

Now considering subgrid solution $\widehat{u}$ as bubble functions, we approximate $u_{ske} = 0$, and also consider $\widehat{v}^{\perp} = 0$ which results in an approximate solution of subgride scales as,

$$\widehat{u}|_K = \tau_K \left(f - \mathcal{L}u_h\right) \tag{3.47}$$

Considering the same discussions as in chapter (2.3) regarding the Fourier analysis of the subgrid problem, the expression of τ for CDR equation can be written in the same way as,

$$\tau = \left[\left(c_1 k^r + s\right)^2 + \left(c_2 \left|\boldsymbol{a}^r\right|\right)^2\right]^{-1/2} \tag{3.48}$$

Finally, the VMS formulation of DG resulting in stabilized DG solution can be expressed as,

$$B_\tau\left(u_h, v_h\right) = L_\tau\left(v_h\right) \qquad v_h \in V_h \tag{3.49}$$

where $B_\tau\left(u_h, v_h\right)$ and $L_\tau\left(v_h\right)$ are the stabilized forms, written as

$$B_\tau\left(u_h, v_h\right) := B_h\left(u_h, v_h\right) + \mathcal{E}\left(u_h, v_h\right) - \left(\mathcal{L}^* v_h, \tau \mathcal{L}u_h\right)_h \tag{3.50}$$

$$L_\tau\left(v_h\right) = L\left(v_h\right) - \left(\mathcal{L}^* v_h, \tau f\right)_h \tag{3.51}$$

For calculation of unknown parameters of the stabilization parameter τ, a simultaneous procedure as in section (2.3.1) have been followed. Then, for example in the case of an isotropic diffusion coefficient and a convection velocity $\boldsymbol{a} = (a, 0)^t$, and for a degree of approximation p, the stabilization parameter is given by,

$$\tau \approx \left[\frac{4k}{\left(\frac{h_1}{p^2}\right)^2} + \frac{2a}{\left(\frac{h_1}{p}\right)}\right]^{-1} \tag{3.52}$$

4

Numerical results

In previous chapters, a DG method was developed and also the CG method was introduced for solving CDR problem. It was discussed that in convection dominated problems, both of the methods may go through numerical instabilities represented as spurious oscillations in the solution of the problem. To overcome this problem, it was discussed that the Variational Multiscale (VMS) method is an option to stabilize these methods. Then the stabilized CG method was introduced and a stabilized DG method was developed.

In the current chapter, some numerical tests have been presented and used to investigate various characteristics of the DG, and stabilized DG solution of the CDR equations. To verify our results, the CG solution of the corresponding examples have been computed and compared to the DG results. Finally, an application-based problem, which is to compute the concentration of fuel in a combustor, has been solved using the developed stabilized DG method.

4.1 Numerical formulation in the transient and nonlinear case

A steady CDR problem was introduced in Chapter (1.1), which has been the basis for the formulations in previous chapters. Let us present a transient CDR problem

consisting with a general nonlinear reaction term, that is,

$$\begin{aligned} &\partial_t u + \mathcal{L}u = f \qquad && in\, \Omega \times (0,T)\,, \\ &u = 0 && on\, \partial\Omega \times (0,T)\,, \\ &u = u_0 && on\, \Omega \times \{0\} \end{aligned} \tag{4.1}$$

where $\mathcal{L}$ is the CDR operator

$$\mathcal{L}u := -k\Delta u + \boldsymbol{a} \cdot \nabla u + R\,(u;\mu)\,, \tag{4.2}$$

Ω is a bounded domain in $\mathbb{R}^d$ with boundary $\partial\Omega$.

Here $R\,(u;\mu)$ is the nonlinear reaction coefficient, μ is a system parameter that will be explained in section (4.3), $k > 0$ is the constant (positive definite) and symmetric diffusion tensor, $\boldsymbol{a} \in \mathbb{R}^d$ the constant velocity field, and $u_0 \in L^2\,(\Omega)$ is the initial condition. This equation models an application-based problem for concentration of fuel in a combustor. In order to solve the proposed equation some steps are required regarding the time integration and also the nonlinearity of the reaction term that will be discussed in the following.

Time integration. There are various schemes proposed for time integration of the transient problems. Some of the well-known methods include, the second order Crank Nicolson scheme, and the Backward Differencing time integration schemes (denoted by BDF). Cranck Nicolson schemes generally contain errors on phase magnitude (if implemented for the wave equation for example) and more accurate on domain magnitude, but in turn the BDF2 schemes are more accurate on phase magnitude though containing error on the domain magnitude. Since having error on phase is much harmful than having error on domain, here we have implemented BDF schemes. Accordingly, the BDF1 time integration scheme for equation 4.1 is defined as,

$$\frac{u^{n+1} - u^n}{\delta t} + \mathcal{L}\left(u^{n+1}\right) = f^{n+1} \tag{4.3}$$

and the same equation using the BDF2 schemes is defined as,

$$\frac{3u^{n+1} - 4u^n + u^{n-1}}{2\delta t} + \mathcal{L}\left(u^{n+1}\right) = f^{n+1} \tag{4.4}$$

where n is the time step and $0 = t^0 < t^1 < \cdots < t^n < \cdots < t^N = t^{final}$, with $0 \leq n \leq N$. It is noticed that the BDF2 is the main scheme used here for the time integration, and BDF1 scheme has been implemented only at the beginning ($t = 0$).

Linearization of the nonlinear reaction term. Because of the existence of a nonlinear reaction, it is required to linearize this term. To this end, the well-known Newton methods have been implemented. Hence, the iterative linearized form of 4.1 at each time step (BDF2 time integration scheme) gives,

$$\begin{aligned} \frac{3u_{i+1}^{n+1} - 4u^n + u^{n-1}}{2\delta t} &- k\Delta u_{i+1}^{n+1} + \boldsymbol{a} \cdot \nabla u_{i+1}^{n+1} && (4.5) \\ &+ R\left(u_i^{n+1}\right) + R'\left(u_i^{n+1}\right)\left(u_{i+1}^{n+1} - u_i^{n+1}\right) = f^{n+1} && (4.6) \end{aligned}$$

Let us to introduce a notation for the iterative solution of the linearized equation at each time step (Nonlinear Transient case) as $u = u_{i+1}^{n+1}$. Then the above expression can be written in a more compact form that represents the algorithmic form of the time integration for the linearized problem, that is,

$$\mathcal{L}(u) := -k\Delta u + \boldsymbol{a} \cdot \nabla u + s_{nt} u = f_{nt} \tag{4.7}$$

where

$$\begin{aligned} s_{nt} &= \left(\frac{3}{2\delta t} + R'\left(u_i^{n+1}\right)\right), \\ f_{nt} &= f^{n+1} + \frac{2u^n}{\delta t} - \frac{u^{n-1}}{2\delta t} - R\left(u_i^{n+1}\right) + R'\left(u_i^{n+1}\right) u_i^{n+1} \end{aligned}$$

Here i is the iteration for linearization at each time step n.

VMS stabilization. Now after deriving the variational formulation of 4.7 and following the same approach introduced in section (3.3) for stabilized DG method, we may write the stabilized DG formulation of the nonlinear transient CDR equation as follows, find $u_h \in V_h$ such that

$$B_\tau(u_h, v_h) = L_\tau(v_h) \qquad v_h \in V_h \tag{4.8}$$

where

$$B_\tau\left(u_h, v_h\right) := B_h\left(u_h, v_h\right) + \mathcal{E}\left(u_h, v_h\right) - \left(\mathcal{L}^* v_h, \tau \mathcal{L} u_h\right)_h$$
$$L_\tau\left(v_h\right) = L_h\left(v_h\right) - \left(\mathcal{L}^* v_h, \tau f_{nt}\right)_h$$

Similar to the procedure in section (2.3) considering the case with convection velocity $\boldsymbol{a} = (a, 0)$, the stabilization parameter is given by,

$$\tau \approx \left[\frac{4k}{\left(\frac{h_1}{p^2}\right)^2} + s_{nt} + \frac{2a}{\left(\frac{h_1}{p}\right)} \right]^{-1} \tag{4.9}$$

4.2 Some simple tests

In previous chapters the numerical solution of CDR problem was proposed and stabilized continuous and discontinuous Galerkin formulations were introduced in particular to deal with convection-dominated problems. In this chapter, some simple tests have been carried out using the proposed DG formulation which has been validated using the results obtained from CG method. In numerical examples at this study, the following has been considered. Peclet number denoted by Pe is a dimensionless number that is commonly used in convection-diffusion problems. In the current discussion, Pe_c is referred to as the cell Peclet number (inside each element) and Pe_L as the domain Peclet number defined as,

$$Pe_c = \frac{|\boldsymbol{a}|\, h}{2k}, \quad and, \quad Pe_L = \frac{|\boldsymbol{a}|\, L}{k} \tag{4.10}$$

where h is the element length, and L is the domain length. In convection dominated problems the Peclet number is large ($Pe \gg 0$) and numerical instabilities occur.

4.2.1 1D convection-diffusion

In this section, some numerical experiments have been conducted for a convection diffusion problem in 1-D and in a convection-dominated regime. The discretization has been carried out by both CG and DG methods and using both unstabilized and stabilized formulations. Also the approximations have been used for orders of $p = 1, \cdots, 4$ (linear, quadratic, cubic, and quartic elements) which shape functions and the gauss rule points have been designed and implemented.

In the following examples it has been considered that our domain is $\Omega = [0, 1]$ and the source term, $f = 1$, h denotes the element size, and p denotes the order of polynomial approximation.

4.2.1.1 Continuous Galerkin results

As a first example the non-stabilized and stabilized CG results have been depicted in figure 4.1.

Since the problem is convection dominated (with a $Pe_c = 30$), which is very greater than one, the CG solution performs spurious oscillations. On the other hand the stabilized results show that using VMS method, the spurious oscillations are disappeared. Furthermore, it is noticed that our stabilization is global and we are not stabilizing locally. Accordingly, the local instabilities that appear in stabilized results, in a very sharp edge, cannot be treated using this method. For that, local mesh refinement or some special treatment such as shock capturing method could be proposed which is beyond the aims of this study.

4.2.1.2 Discontinuous Galerkin results

The problem that was investigated in previous section is recalled here and the DG discretization has been used to solve it. The problem has been solved for non-stabilized and stabilized DG methods using proposed formulations 3.40, and 3.49 respectively. According to these formulations, it is observed that there is a coefficient δ, so-called penalty parameter, in the convection and diffusion flux continuity terms which has not been assigned any specific values, and will be shown to be a crucial parameter. As a matter of fact, the calculation of the coefficient δ is not easy and is always a case that needs considerations (e.g. using error analysis).

Let us define the penalty parameter as $\delta = \alpha h$ where h is the element size and α is a coefficient that will be discussed later. Referring to the figure 3.2, the definition of $\delta = \alpha h$ is equivalent to taking a distance from the element edge inside each element depending on a coefficient α. Here we have selected the values of $\alpha < 0.5$ which looking back to the figure 3.2 makes sense (δ with a limit of $0.5h$).

Figures 4.2, illustrate the DG solution of the proposed problem in non-stabilized and stabilized cases for different orders of polynomial approximation, and considering different values of α coefficient.

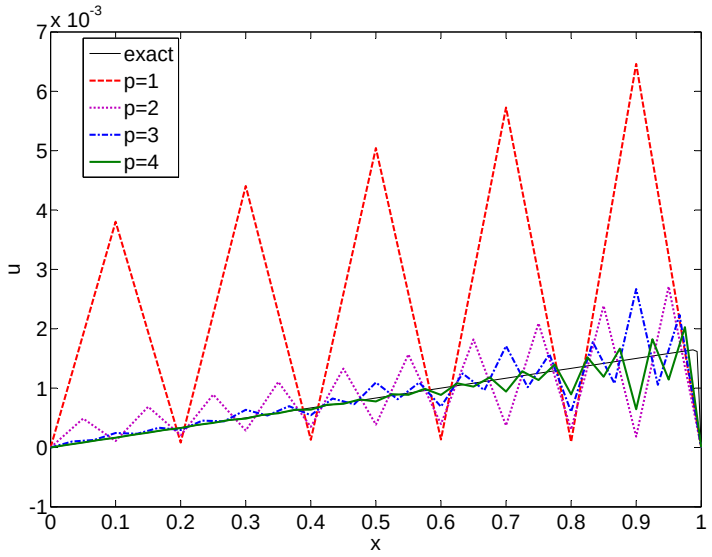

(a) Non-stabilized CG results

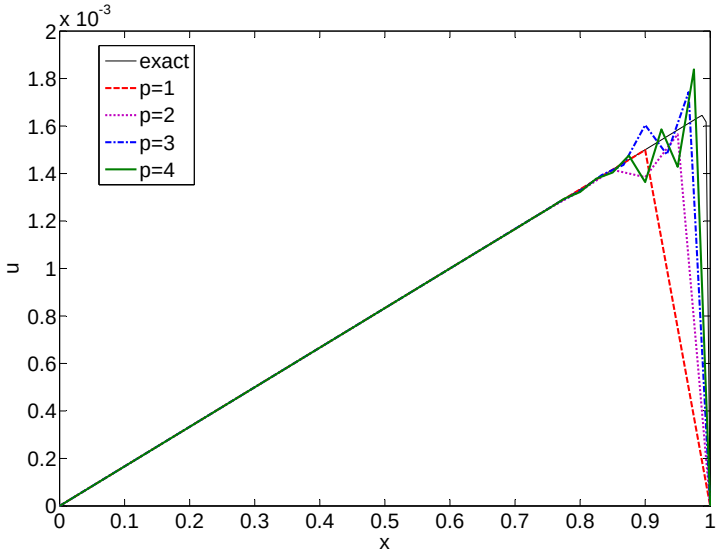

(b) Stabilized CG results

Figure 4.1: CG results, 10 elements, $Pe_c = 30$

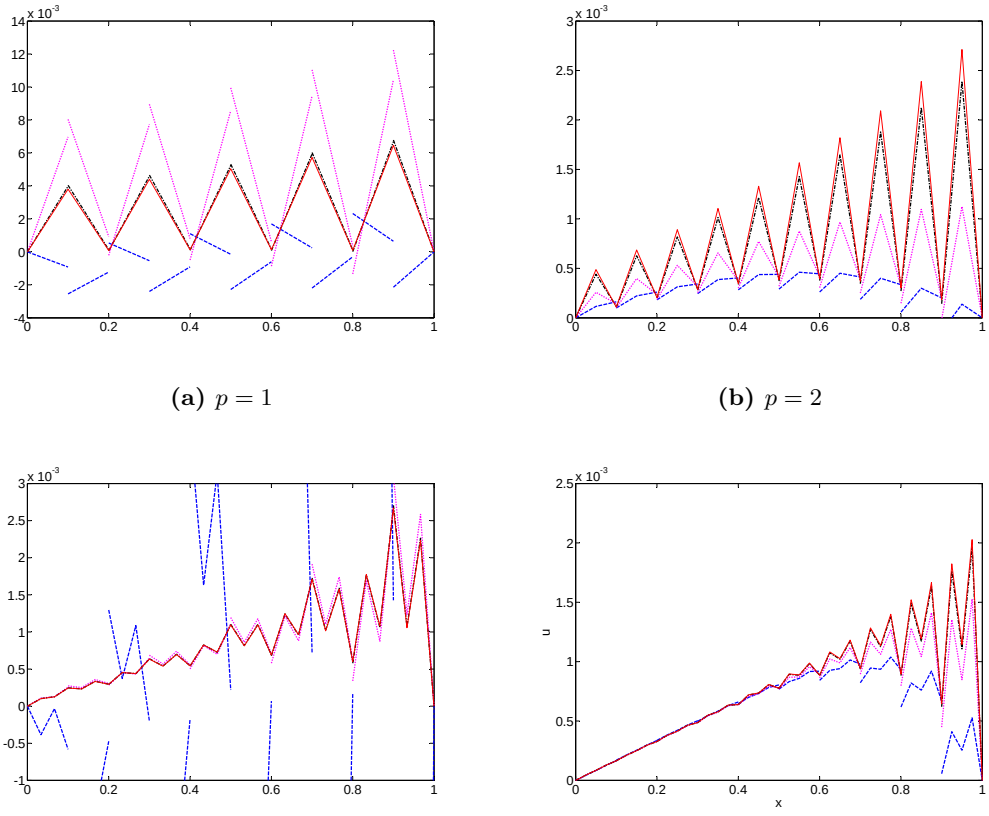

(a) $p = 1$ **(b)** $p = 2$

(c) $p = 3$ **(d)** $p = 4$

Figure 4.2: non-stabilized DG results compared to CG results, $Pe_c = 30$. dashed blue line: $\alpha = 0.05$, dotted magenta line: $\alpha = 0.005$, dashed-dotted black line: $\alpha = 0.0005$, and solid red line: CG solution.

Now let us analyze the effect of the penalty coefficient on our DG solution using these figures and and by looking back to our DG formulation 3.40. It is observed that this formulation contain two terms which are dependent on the penalty parameter δ, that is, the diffusion flux continuity term,

$$\frac{k}{\delta}\left(\llbracket \boldsymbol{n} u_h \rrbracket, \llbracket \boldsymbol{n} v_h \rrbracket\right)_{\mathcal{E}}, \tag{4.11}$$

and the convection flux continuity term,

$$\frac{\delta}{2}\left(\llbracket \boldsymbol{n} \cdot \nabla v_h \rrbracket, \llbracket \boldsymbol{n} \cdot \boldsymbol{a} u_h \rrbracket\right)_{\mathcal{E}}.$$

reminding that $\delta = \alpha h$ was defined before.

Assume values of the penalty parameter when $\alpha \to 0$. In this case and when k is fixed (for $Pe < 1$ or $Pe > 1$ and of course being sure that $Pe \to \infty$ is not the case), the formulation will enforce, strongly, the continuity. For these values of α the same stability problems as in the continuous case may be encountered. This may imply that the DG results are performing in continuous space. Whereas if we assume comparatively large (critical) values of the penalty parameter when $\alpha \to \alpha_c$ (with critical coefficient $\alpha_c = 0.5$ in limit) when $k \to 0$, excessive continuity will be enforced in the direction of convection velocity $\boldsymbol{a}$ which can be manifested with bigger jumps over the element edges. Another important issue that must be considered is in a case when $k \to 0$ and $\alpha \to 0$ which would impose a $\frac{0}{0}$ delimma and therefore must be avoided by appropriate selection of α value. However, by proper selection of the α in that case, either of the fist or second cases discussed above could be anticipated depending on which one of the continuity terms dominates the other.

In fact this can already be checked from the same figures in 4.2 or looking into the left column in figures 4.4, 4.5, and 4.6. When $\alpha = 0.05$ excessive continuity has been imposed in the direction of $\boldsymbol{a}$ and the results represent bigger jumps and not in a good agreement with CG results. On the other hand, when $\alpha = 0.0005$ continuity has been imposed strongly and the resulting DG solution performs close to continuous space as we can see that the CG and DG results are perfectly matching in this case. Also, it is observed that as it was predicted the same stability problems in CG are appearing when continuity is enforced strongly. Furthermore, one may ask to select values of $\alpha > 0.5$. In the case of 1D, quite similar results have been achieved as the previous case but the value of α in this case ($\alpha > 0.5$) play a reverse role compared to the previous case ($\alpha < 0.5$). The reason can be clearly explained looking back to above terms and considering the same explanations as previous case. In figures within 4.3, the results for non-stabilized DG using values of $\alpha > 0.5$ has been depicted and compared to CG results.

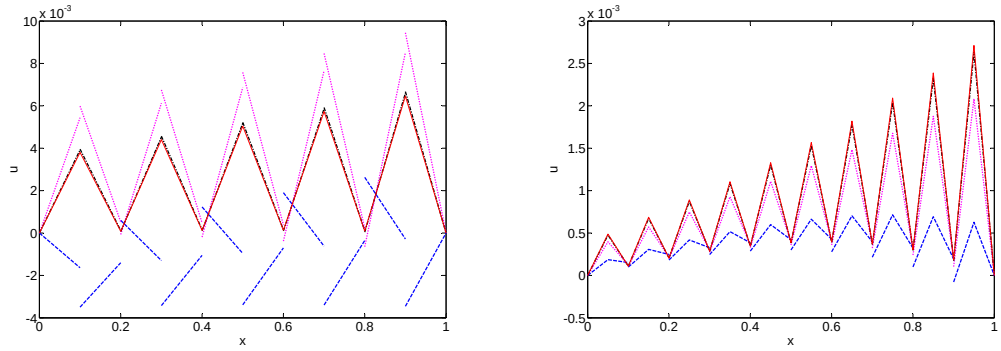

(a) $p = 1$ **(b)** $p = 2$

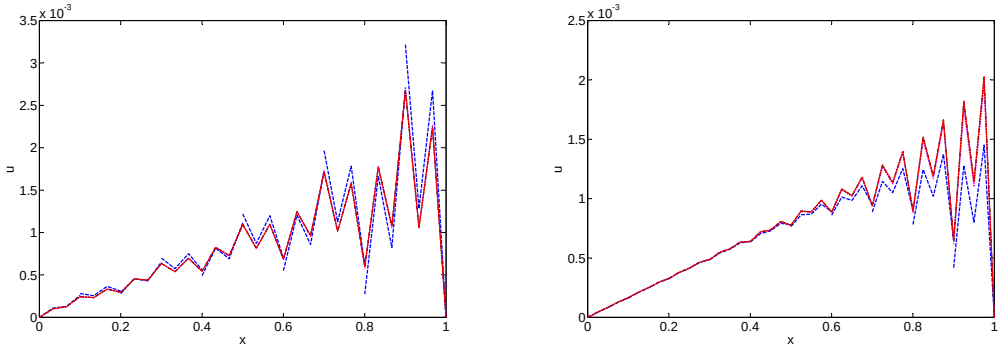

(c) $p = 3$ **(d)** $p = 4$

Figure 4.3: non-stabilized DG results compared to CG results, $Pe_c = 30$. dashed blue line: $\alpha = 1$, dotted magenta line: $\alpha = 10$, dashed-dotted black line: $\alpha = 100$, and solid red line: CG solution.

To overcome the problems occurred with the choice of penalty parameter, one possibility is to use the same stabilization strategy for discontinuous interpolants as for continuous ones. As explained in Chapter (3.3), the stabilization method we have implemented is the VMS method. In figures 4.4 for $\alpha = 0.05$, 4.5 for $\alpha = 0.005$, and 4.6 for $\alpha = 0.0005$, stabilized results have been compared to those of non-stabilized ones for $p = 1, \cdots, 4$.

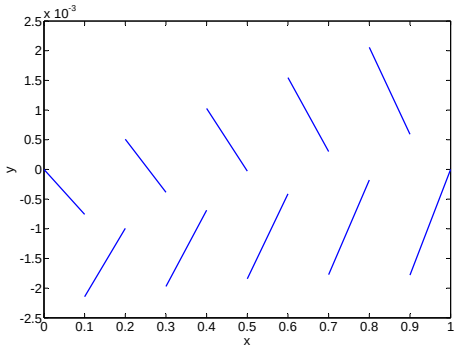

(a) non-stabilized DG, $p = 1$

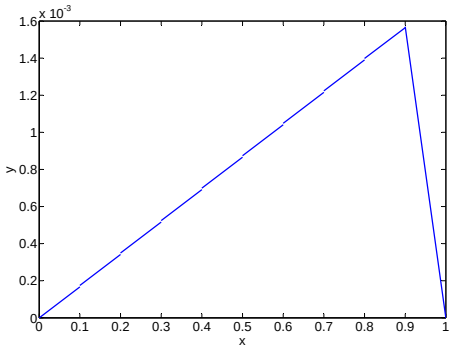

(b) stabilized DG, $p = 1$

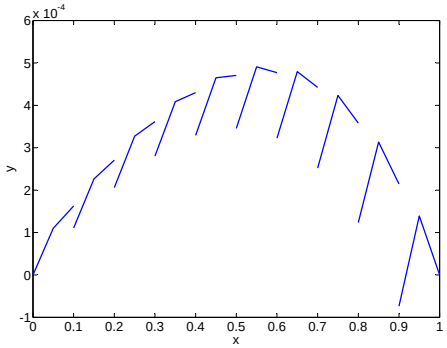

(c) non-stabilized DG, $p = 2$

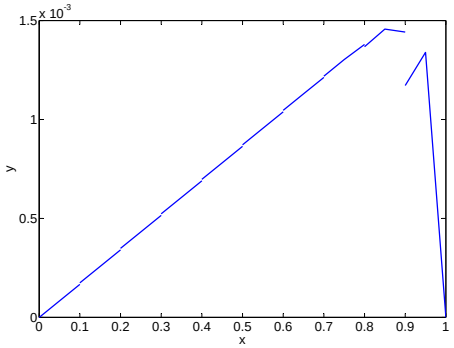

(d) stabilized DG, $p = 2$

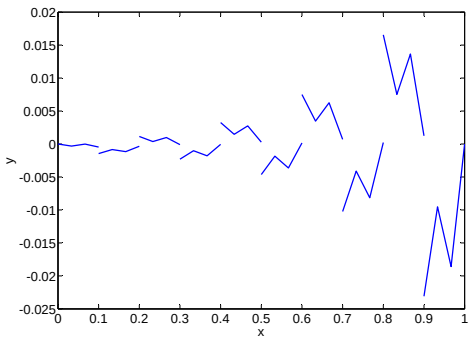

(e) non-stabilized DG, $p = 3$

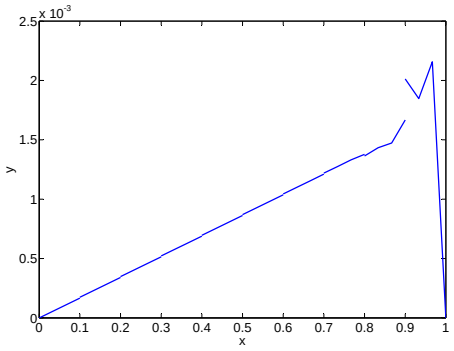

(f) stabilized DG, $p = 3$

Figure 4.4

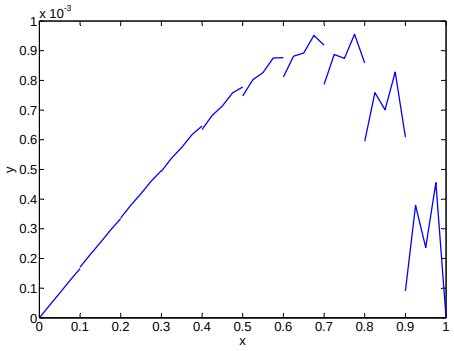

(g) non-stabilized DG, $p = 4$

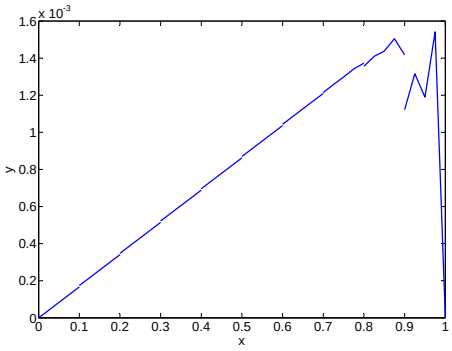

(h) stabilized DG, $p = 4$

Figure 4.4: DG solution, 10 elements, $Pe_c = 30$, with $\alpha = 0.05$

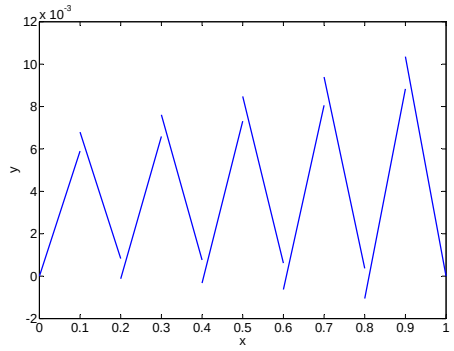

(i) non-stabilized DG, $p = 1$

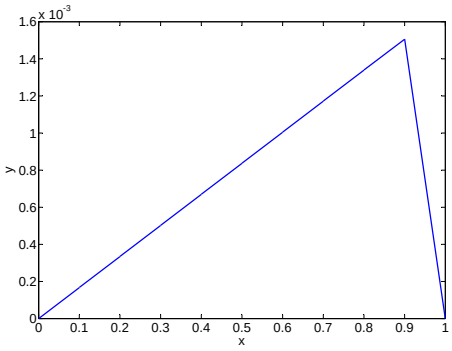

(j) stabilized DG, $p = 1$

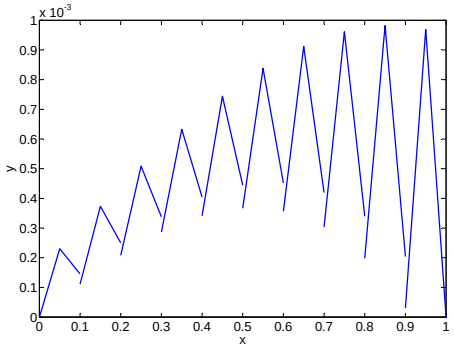

(k) non-stabilized DG, $p = 2$

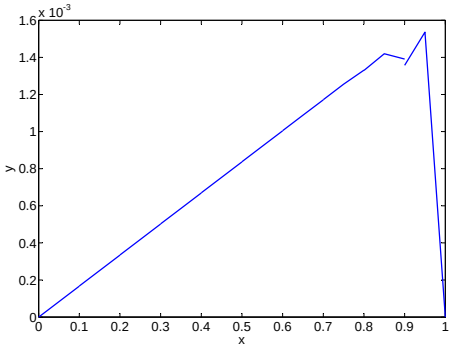

(l) stabilized DG, $p = 2$

Figure 4.5

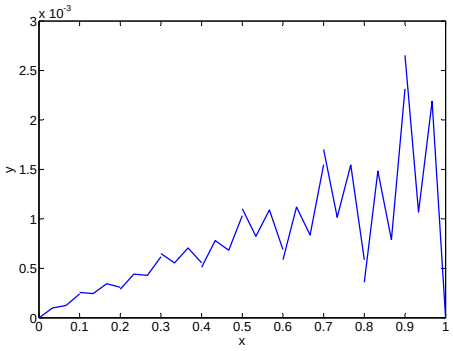

(m) non-stabilized DG, $p = 3$

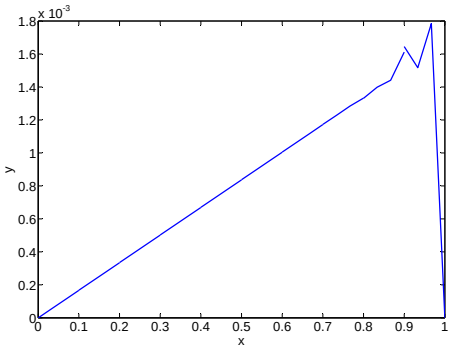

(n) stabilized DG, $p = 3$

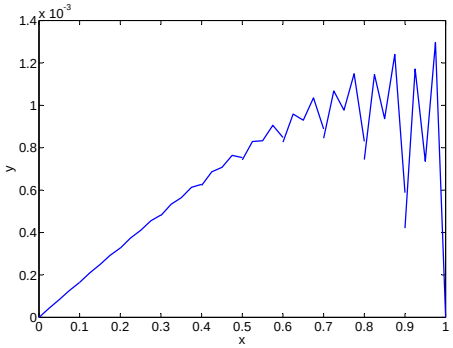

(o) non-stabilized DG, $p = 4$

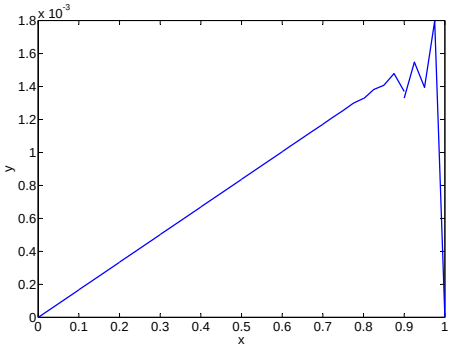

(p) stabilized DG, $p = 4$

Figure 4.5: DG solution, 10 elements, $Pe_c = 30$, with $\alpha = 0.005$

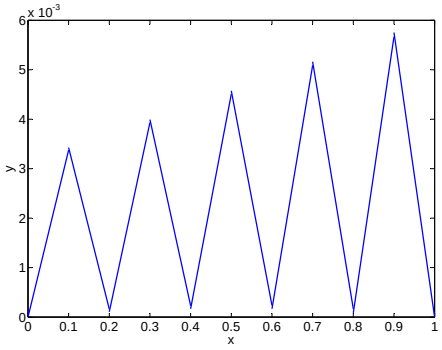

(q) non-stabilized DG, $p = 1$

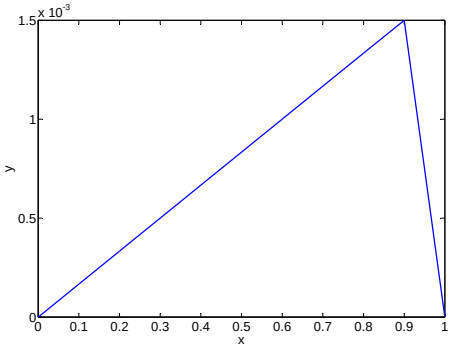

(r) stabilized DG, $p = 1$

Figure 4.6

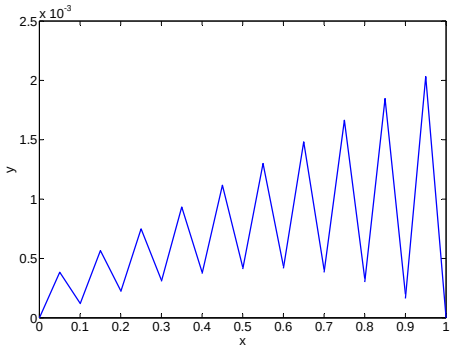

(s) non-stabilized DG, $p = 2$

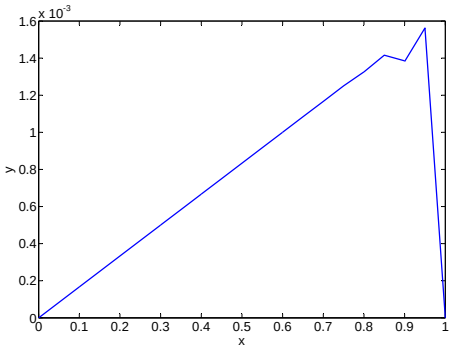

(t) stabilized DG, $p = 2$

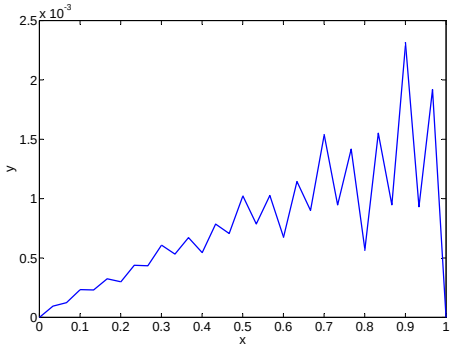

(u) non-stabilized DG, $p = 3$

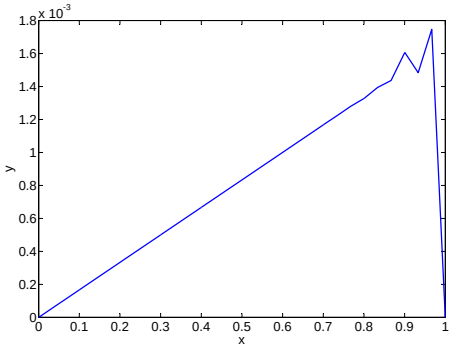

(v) stabilized DG, $p = 3$

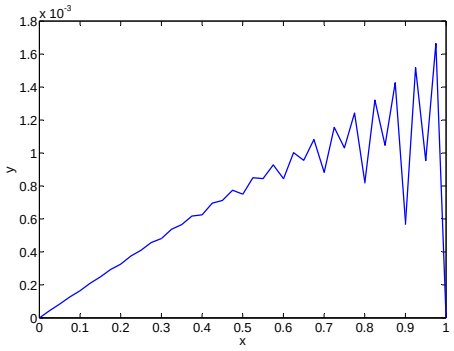

(w) non-stabilized DG, $p = 4$

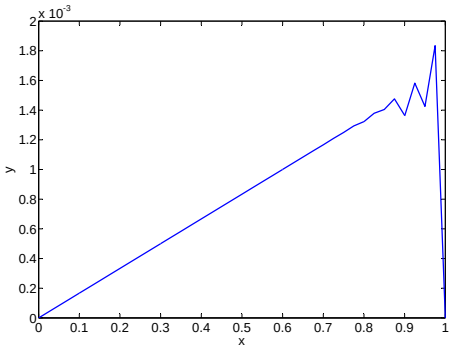

(x) stabilized DG, $p = 4$

Figure 4.6: DG solution, 10 elements, $Pe_c = 30$, with $\alpha = 0.0005$

Some interesting observations have been made through these results. The figures on left side show the non-stabilized DG solution for different values of the penalty co-

efficient δ (based on α). The figures on the right side are the stabilized results for the same problem. An important point that can be inferred from these results is regarding the robustness of the DG methods. As it was explained before, DG methods are felt to have the advantage of robustness due to their built-in stability, especially for first order polynomial approximations. But with respect to these results, depending on the value of the penalty parameter, the DG results either perform spurious oscillations similar to the CG case or produce results that might be inaccurate (with considerable jumps in results which would be visible especially when less number of elements implemented). Furthermore these instabilities occur within both of the low order and high order approximations ($p = 1, \cdots, 4$). This might imply the need for stabilization of the DG method.

The most interesting observation from these examples is that, we show the benefits of adding stabilization to the original DG formulation. According to the stabilized results, no spurious oscillations are appearing (unless a local instability appearing in the sharp edge which cannot be treated by our global stabilization scheme and needs to be treated by local mesh refinement or some special treatment such as shock capturing method). Without adding the stabilization term in convective dominated flows, the solution exhibits a strong dependence on the penalty parameter through the coefficient α that enforces weak continuity of the unknown. By adding the stabilization term the solution is virtually insensitive to this parameter.

4.2.2 2D convection-diffusion

In previous section, some numerical experiments were carried out in 1D case which were followed by some interesting observations regarding the penalty parameter and the need for stabilization of DG method. In the current section, some numerical examples have been presented implementing non-stabilized and stabilized CG and DG solutions in 2D. It is assumed that the source term $f = 1$. A 2D domain $\Omega = [0, 1] \times [0, 1]$ has been considered for all the cases. The boundary conditions are considered either

homogeneous or the one defined as follows,

$$\begin{cases} u(x,0) = u(x,1) = u(1,y) = 0 \\ u(0,y) = 0 \quad when \quad |y-0.5| > 0.125 \\ u(0,y) = 1 \quad when \quad |y-0.5| < 0.075 \\ u(0,y) = 20\,(y-0.375) \quad when \quad y \geq 0.375,\ y \leq 0.425 \\ u(0,y) = 20\,(0.625-y) \quad when \quad y \geq 0.575,\ y \leq 0.625 \end{cases}$$

which has been visualized in figure 4.7.

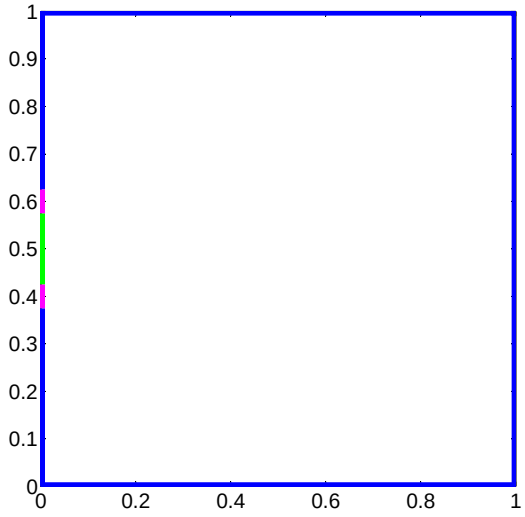

Figure 4.7: Boundary conditions, blue: $u = 0$, green: $u = 1$, magenta: functions of y as defined

The experiments have been carried out for, unstructured and structured triangulars, and structured quadrilaterals. Polynomial approximations of the order $p = 1, \cdots, 4$ i.e. linear, quadratic, cubic, and quartic elements have been implemented in our calculations. To this end, the corresponding shape functions over the elements were built and appropriate gauss rules were implemented for integrations. Noting that the higher order elements were built such that their Jacobian of transformation (from reference to physical element) would be linear. In figure 4.8, some sample domain meshing including unstructured and structured triangular mesh, and quadrilateral mesh has been represented. Also figures within 4.9, are schematic view of part of the mesh depicting the corresponding element's polynomial degree of approximation.

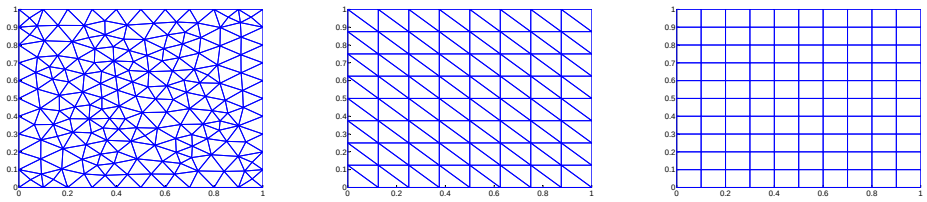

(a) An unstructured triangular mesh

(b) An structured triangular mesh

(c) A quadrilateral mesh

Figure 4.8: A schematic view of the domain partitioned using different types of meshing

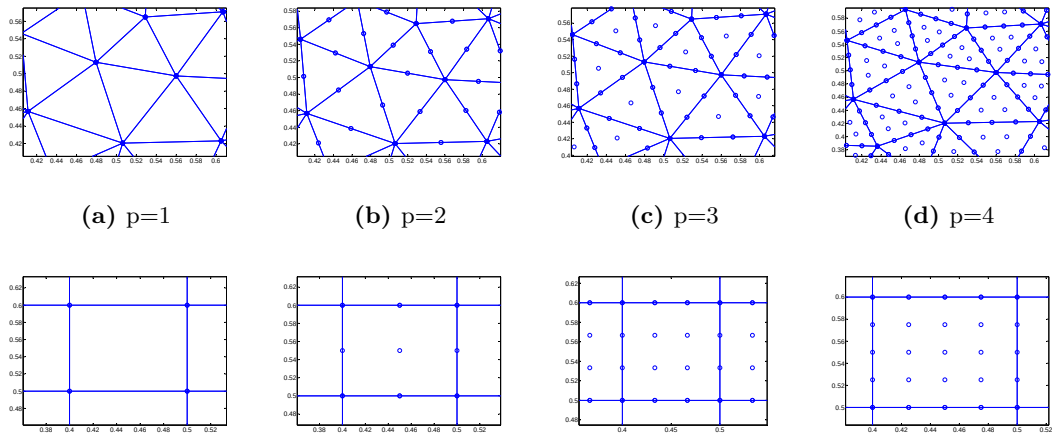

(a) p=1 **(b)** p=2 **(c)** p=3 **(d)** p=4

(e) p=1 **(f)** p=2 **(g)** p=3 **(h)** p=4

Figure 4.9: A schematic view of part of the unstructured triangular mesh, and structured quadrilateral mesh, p is the polynomial order of approximation

4.2.2.1 Continuous Galerkin results

As a first example (figure 4.10) a convection-diffusion problem has been solved using non-stabilized CG approach. Since $Pe_c \ll 0$ the results are stable and there has been no need for stabilization.

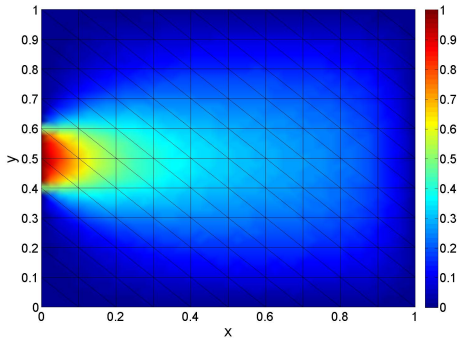

(a) CG, $Pe_c = 0.5$, Structured triangular mesh, 20 elements on each side, $p = 4$

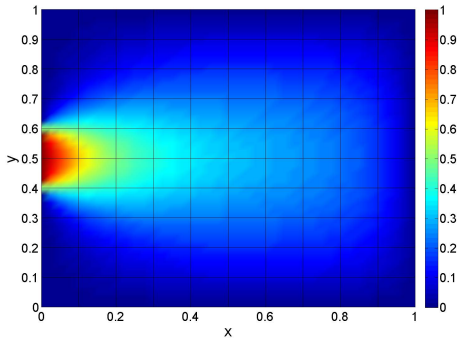

(b) CG, $Pe_c = 0.5$, quadrilateral mesh, 10 elements on each side, $p = 4$

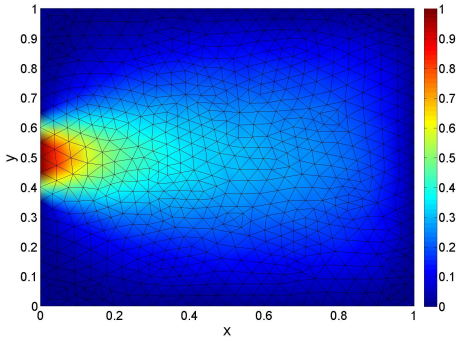

(c) CG, $Pe_{c,min} = 0.1625$, Unstructured triangular mesh, a total of 1312 elements, $p = 1$

Figure 4.10: non-stabilized CG solution for different meshes, in all figures original mesh has been represented

Now let us consider a convection-dominated case with $Pe \gg 0$. In figure 4.11, some of the results for the proposed problem can be observed. The problem has been solved using structured triangular elements and quadrilateral elements, and in non-stabilized and stabilized cases.

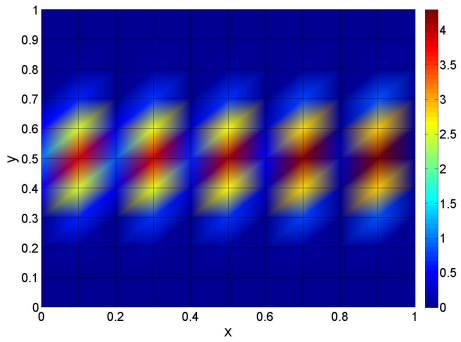

(a) CG, non-stabilized, quadrilaterals with $p = 1$, $Pe_c = 50$

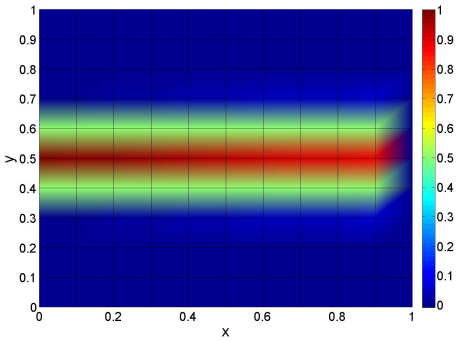

(b) CG, stabilized, quadrilaterals with $p = 1$, $Pe_c = 50$

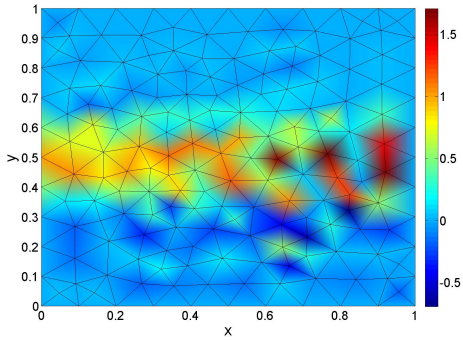

(c) CG, non-stabilized, unstructured tringulars with $p = 1$ ($n_{tot} = 328$), $Pe_{c,min} = 57$

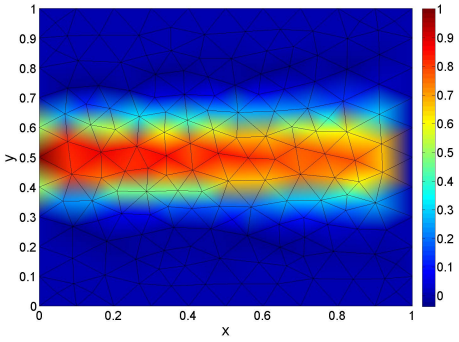

(d) CG, stabilized, unstructured tringulars with $p = 1$ ($n_{tot} = 328$), $Pe_{c,min} = 57$

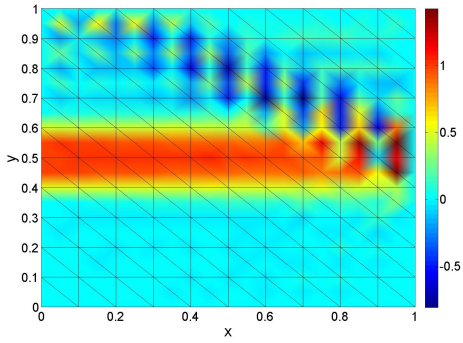

(e) CG, non-stabilized, triangulars with $p = 2$, $Pe_c = 50$

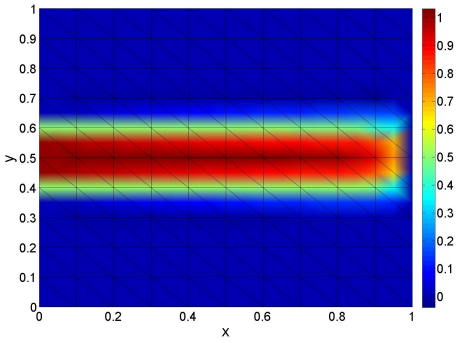

(f) CG, stabilized, triangulars with $p = 2$, $Pe_c = 50$

Figure 4.11

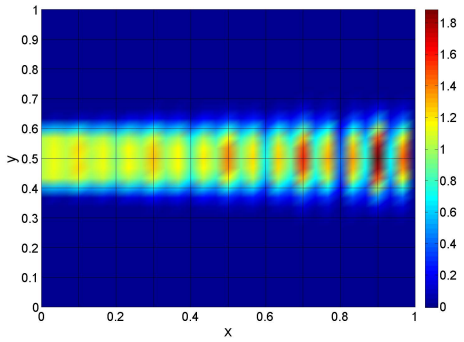

(g) CG, non-stabilized, quadrilaterals with $p = 3$, $Pe_c = 50$

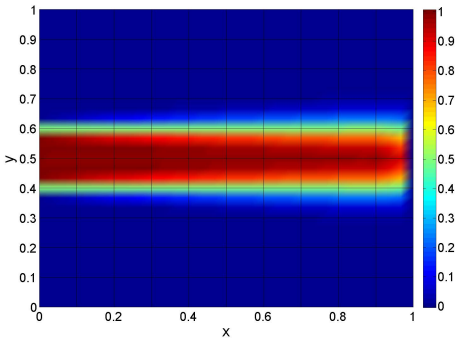

(h) CG, stabilized, quadrilaterals with $p = 3$, $Pe_c = 50$

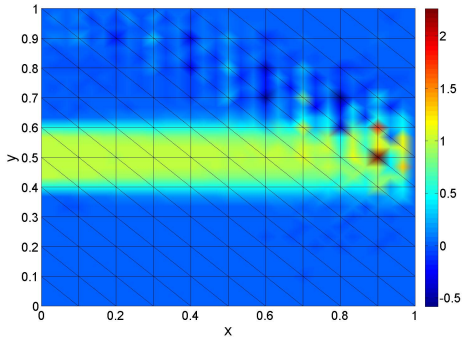

(i) CG, non-stabilized, triangulars with $p = 3$, $Pe_c = 50$

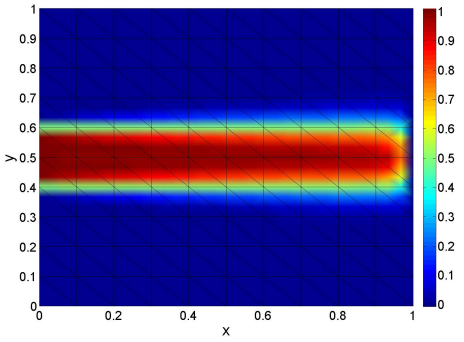

(j) CG, stabilized, triangulars with $p = 3$, $Pe_c = 50$

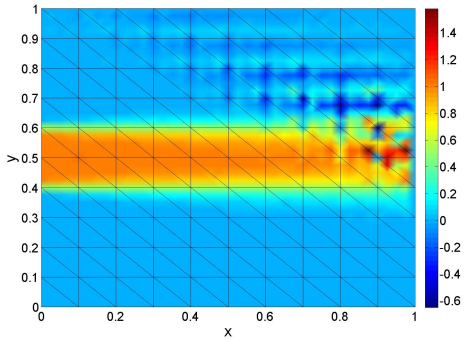

(k) CG, non-stabilized, triangulars with $p = 4$, $Pe_c = 50$

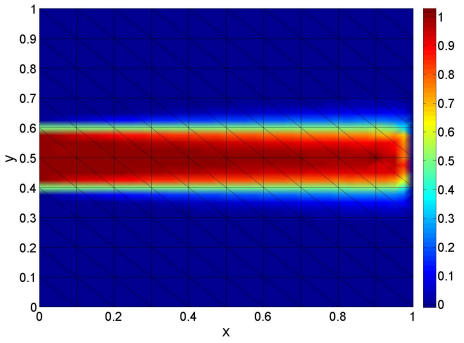

(l) CG, stabilized, triangulars with $p = 4$, $Pe_c = 50$

Figure 4.11

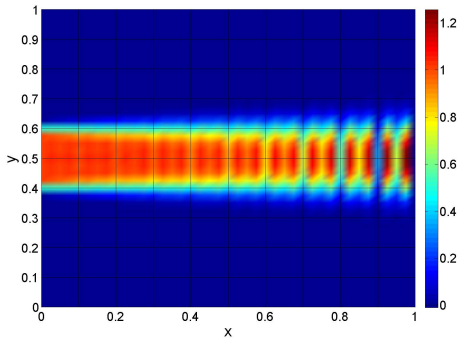

(m) CG, non-stabilized, quadrilaterals with $p = 4$, $Pe_c = 50$

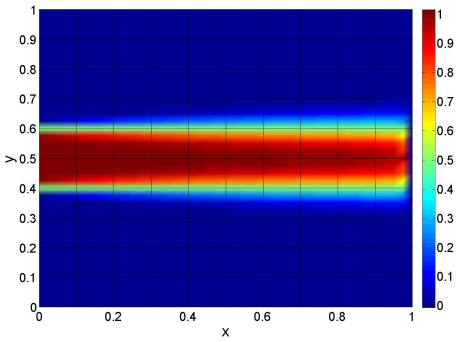

(n) CG, stabilized, quadrilaterals with $p = 4$, $Pe_c = 50$

Figure 4.11: convection-dominated samples, CG results for non-stabilized and stabilized cases, quadrilaterals with 10 elements on each side, and structured triangulars with 20 elements on each side, in all the figures original mesh has been represented

These simple examples demonstrate the inconsistency problems arising in convection-dominated regime. Also, the stabilized results show that using VMS, the results have become stabilized and the spurious oscillations are damped out.

4.2.2.2 Discontinuous Galerkin results

In this section a set of numerical examples similar to the ones in CG case have been presented. Non-stabilized and stabilized DG methods have been implemented in order to discretize the problem. Different orders of approximations from linear to quartic ($p = 1, \cdots, 4$) have been considered using unstructured and structured triangulars and also quadrilateral elements. The previous assumptions regarding the domain etc are also valid in this case. In order to implement the DG formulation 3.40, we have considered the penalty parameter $\delta = \alpha h_{orth}$ where α is a parameter similar to the one defined in 1D case, and h_{orth} is a characteristic length. Since two neighboring elements sharing an edge may have different sizes, there is a need to define a common length for h_{orth} implemented for both of the fluxes coming from these elements on the sharing edge. Therefore, h_{orth} has been taken equivalence to a distance between the barycenters of two neighbor elements and is orthogonal to the sharing edge (figure 4.12).

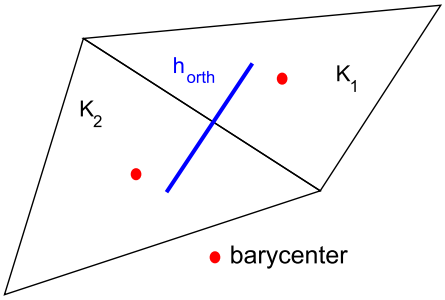

Figure 4.12: two neighboring elements and their h_{orth}

With these definitions, let us first start with some Convection-Diffusion (CD) problems which are stable and do not require stabilization. To this end, two types of boundary conditions, homogeneous and also the general one specified at the beginning of the section (4.2.4) have been considered. In figures 4.13, a pure diffusion case has been considered with homogeneous boundary conditions (to test the simplest case). Following that, figures 4.14 represent a set of examples for CD problem with non-homogeneous boundaries which are also in a stable regime.

As it was mentioned previously instabilities are present in convection-dominated regimes in CD problems. In figures 4.15, 4.16, 4.17, and 4.18 several numerical examples have been represented using non-stabilized and stabilized DG formulations in a convection-dominated case. Different types of elements including, structured and unstructured triangulars, and also quadrilaterals have been implemented to discretized the problem. Instabilities are clearly visible in all the cases, whereas the results for the stabilized cases do not perform any spurious oscillations. There have been some very interesting observations which confirm our results in previous section for 1D case. Regarding the penalty parameter α in our DG formulation 3.40, several different values have been tried in the aforementioned figures. It was discussed in section (4.2) that the values of the $\alpha < 0.5$ are the ones that based on the derivation of our DG formulation make more sense and can be confirmed here in 2D case as well (values used are between $0.00001 \leq \alpha \leq 0.01$). With the same discussion in previous section for 1D case and looking back to the convection and diffusion continuity terms in equation 3.40 as shown in equation 4.11, we can analyze our results in shown in the current figures in 2D similarly.

When $\alpha \to 0$ while k is fixed and considering $Pe < 1$ or $Pe > 1$ knowing that $Pe \to$

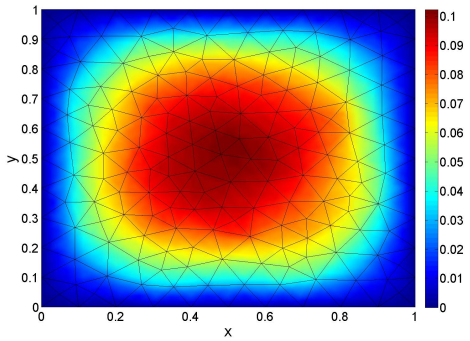

(a) $\alpha = 0.01$, non-stabilized unstructured tringulars with $p = 4$, with $n_{tot} = 328$ elements

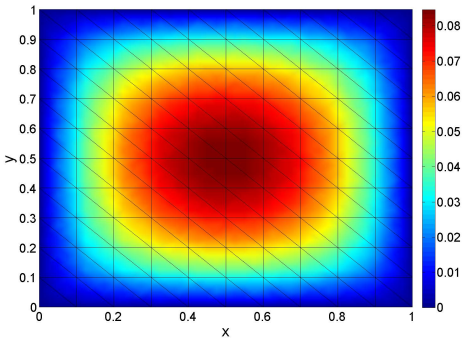

(b) $\alpha = 0.01$, non-stabilized structured tringulars with $p = 4$, with 20 elements on each side

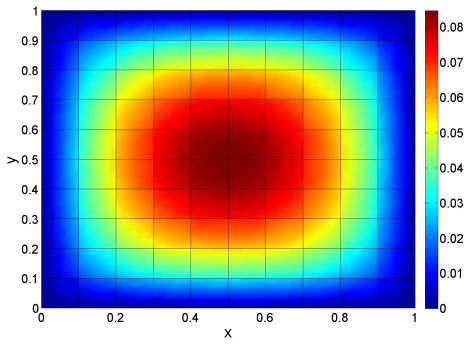

(c) $\alpha = 0.01$, non-stabilized quadrilaterals with $p = 4$, with 10 elements on each side

Figure 4.13: DG, homogeneous boundary condition, stable case, original mesh represented

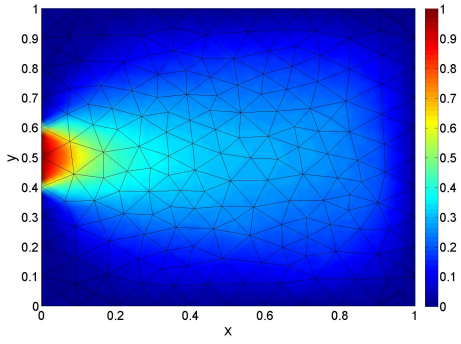

(a) $\alpha = 0.01$, non-stabilized unstructured tringulars with $p = 4$, $Pe_{c,min} = 0.324$

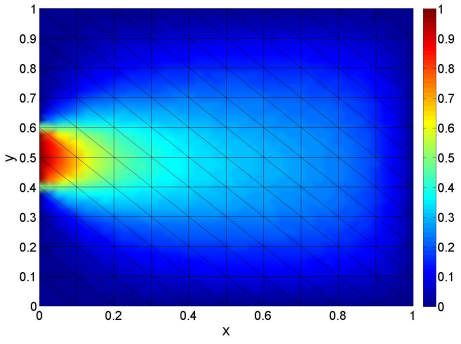

(b) $\alpha = 0.01$, non-stabilized structured tringulars with $p = 4$, $Pe_{c,min} = 0.5$

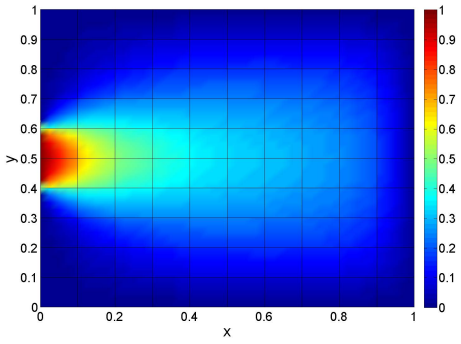

(c) $\alpha = 0.01$, non-stabilized quadrilaterals with $p = 4$, $Pe_c = 0.5$

Figure 4.14: DG, stable case, original mesh represented

∞ is not the case, continuity is strongly enforced by the formulation. Then the DG results may perform in continuous space and the same stability problems encountered in the case of CG results may be expected in DG results in this case. Whereas for comparatively large (critical) values of the penalty parameter when $\alpha \rightarrow \alpha_c$ (with critical coefficient $\alpha_c = 0.5$ in limit) when $k \rightarrow 0$, excessive continuity is enforced in the direction of convection velocity which may be characterized by bigger jumps across the interior boundaries as it can be observed in the figures. It is noticed that when $k \rightarrow 0$ and $\alpha \rightarrow 0$ the $\frac{0}{0}$ delimma will be expected which must be treated carefully by appropriate choice of α. After the proper selection of α parameter the results might behave similar to the cases discussed above.

These discussions can be checked from the same results in figures 4.15, 4.16, 4.17, and 4.18 compared to CG results in figure 4.11. Comparing the non-stabilized DG solutions with $\alpha = 0.0001$ or $\alpha = 0.00001$ to the CG results with similar conditions (the same polynomial approximation, Pe number and so on), it is observed that by decreasing the penalty parameter ($\alpha \rightarrow 0$), the DG results seem to be performing in continuous space especially when $\alpha = 0.00001$ the CG and DG results are perfectly comparable. In order to check, for example see figure 4.15e compared to 4.11c, figure 4.16e compared to 4.11e, figures 4.17e and 4.17g compared to figures 4.11g and 4.11i respectively, and figures 4.18e and 4.18g compared to figures 4.11k and 4.11m respectively. On the other hand, for larger values of penalty parameter such as $\alpha = 0.01$ bigger jumps are visible in the figures and the DG results are not in good agreement with those of CG ones.

To deal with the problems arising from the choice of the stabilization parameter, a possibility is to use a stabilized strategy, similar to continuous case, for Discontinuous interpolations. As it was discussed in section (3.3), VMS method have been implemented to achieve a stabilized DG formulation as in equation 3.49. Now let us look back into the same figures 4.15, 4.16, 4.17, and 4.18. On the right column of the figures, the stabilized results have been represented for all the cases with different elements and interpolations using different values for α. A very interesting conclusion can be understood by comparing the stabilized results and their non-stabilized solution, i.e. the stabilized results for each degree of interpolation behave very similarly, seeming to be independent from the values of α. This has been already observed in 1D case in previous section which can be now confirmed using these results in 2D. In non-stabilized

cases the DG results are strongly dependent on the penalty parameter by α, whereas in stabilized DG results the solution is virtually insensitive to the parameter α. This may imply some benefits of stabilization in DG methods.

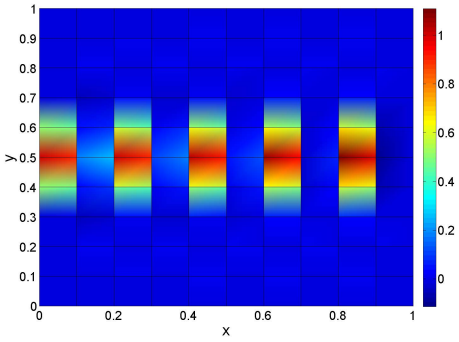

(a) $\alpha = 0.01$,non-stabilized quadrilaterals with $p = 1$, $Pe_c = 50$

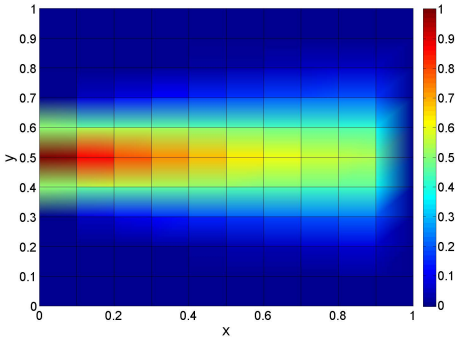

(b) $\alpha = 0.01$, stabilized quadrilaterals with $p = 1$, $Pe_c = 50$

Figure 4.15

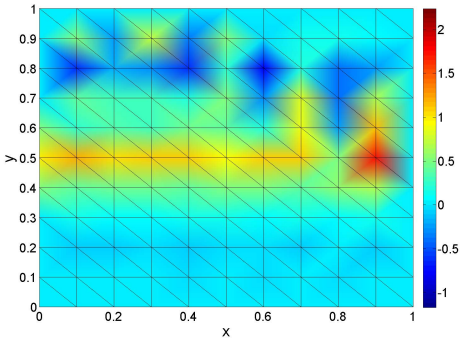

(c) $\alpha = 0.001$,non-stabilized structured tringulars with $p = 1$, $Pe_c = 50$

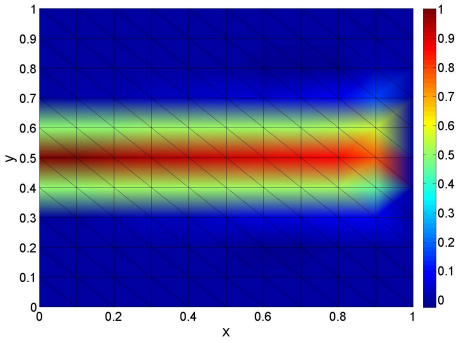

(d) $\alpha = 0.001$, stabilized structured tringulars with $p = 1$, $Pe_c = 50$

Figure 4.15

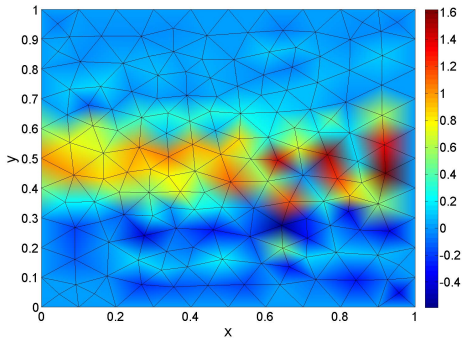

(e) $\alpha = 0.0001$,non-stabilized unstructured tringulars with $p = 1$, $Pe_c = 57$

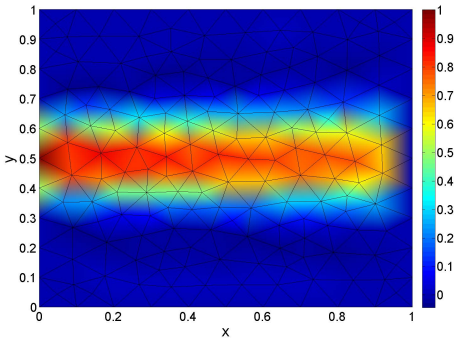

(f) $\alpha = 0.0001$, stabilized unstructured tringulars with $p = 1$, $Pe_c = 57$

Figure 4.15: DG solution, $p = 1$, convection-dominated regime, quadrilaterals elements are with 10 elements on each side, structured triangulars with 20 elements on each side, and unstructured tringulars with total of 328 elements. The original mesh is represented within each figure

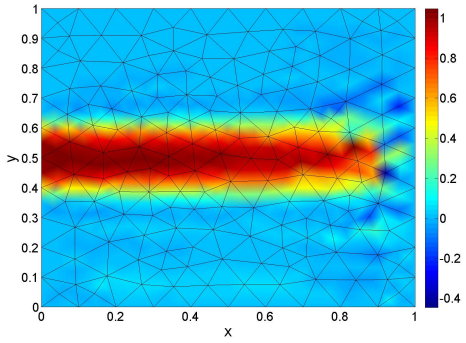

(a) $\alpha = 0.01$,non-stabilized unstructured tringulars with $p = 2$, $Pe_c = 57$

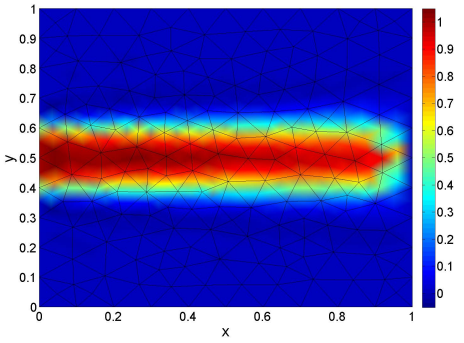

(b) $\alpha = 0.01$, stabilized unstructured tringulars with $p = 2$, $Pe_c = 57$

Figure 4.16

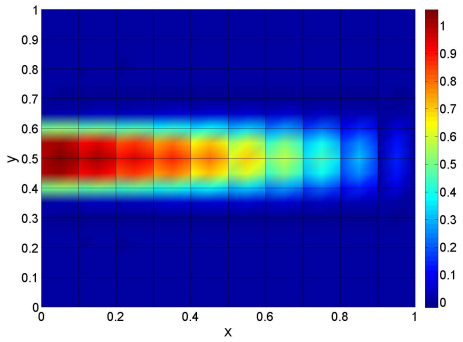

(c) $\alpha = 0.001$,non-stabilized quadrilaterals with $p = 2$, $Pe_c = 50$

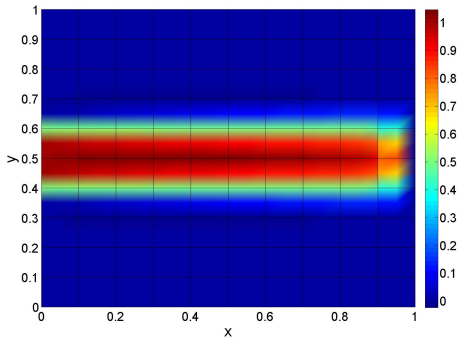

(d) $\alpha = 0.001$, stabilized quadrilaterals with $p = 2$, $Pe_c = 50$

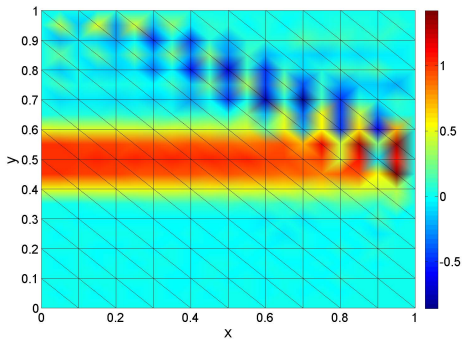

(e) $\alpha = 0.0001$, non-stabilized structured tringulars with $p = 2$, $Pe_c = 50$

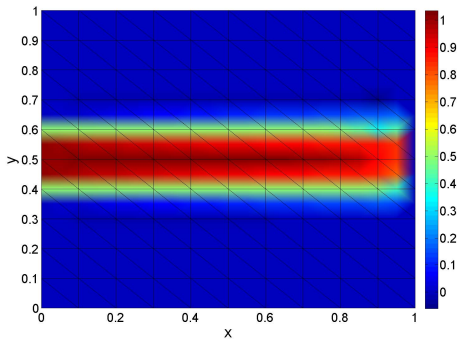

(f) $\alpha = 0.0001$, stabilized structured tringulars with $p = 2$, $Pe_c = 50$

Figure 4.16: DG solution, $p = 2$, convection-dominated regime, quadrilaterals elements are with 10 elements on each side, structured triangulars with 20 elements on each side, and unstructured tringulars with total of 328 elements. The original mesh is represented within each figure

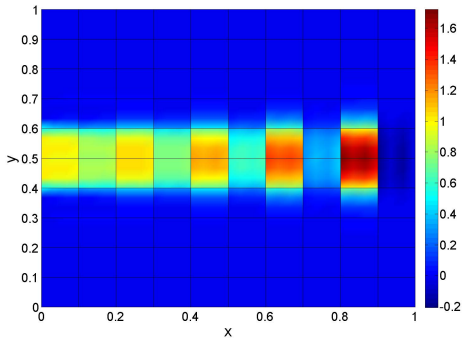

(a) $\alpha = 0.01$,non-stabilized quadrilaterals with $p = 3$, $Pe_c = 50$

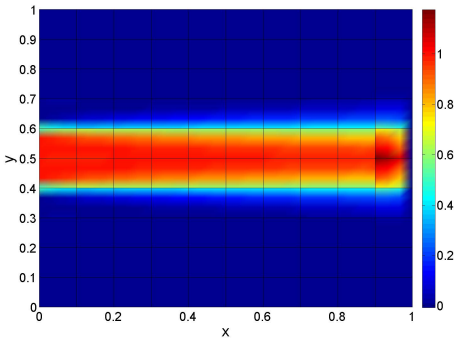

(b) $\alpha = 0.01$, stabilized quadrilaterals with $p = 3$, $Pe_c = 50$

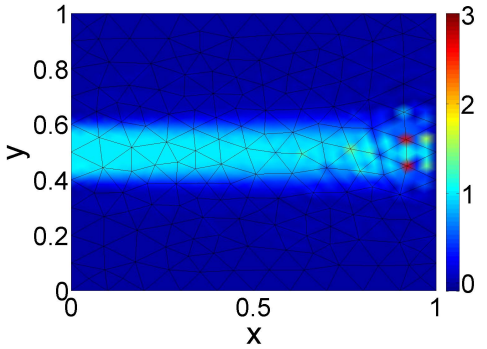

(c) $\alpha = 0.001$,non-stabilized unstructured tringulars with $p = 3$, $Pe_c = 57$

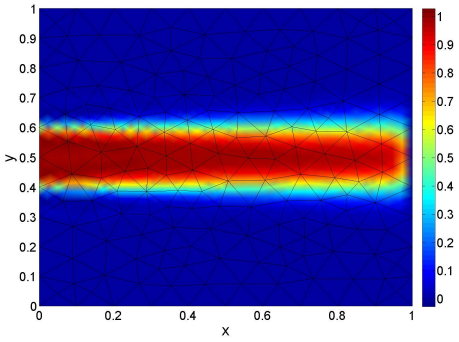

(d) $\alpha = 0.001$, stabilized unstructured tringulars with $p = 3$, $Pe_c = 57$

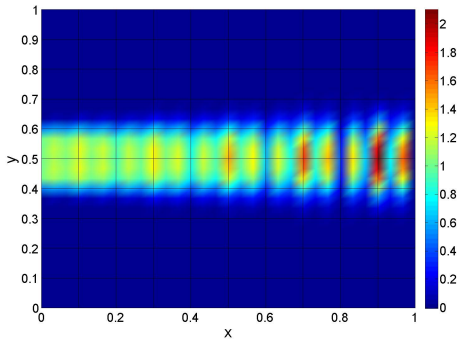

(e) $\alpha = 0.0001$,non-stabilized quadrilaterals with $p = 3$, $Pe_c = 50$

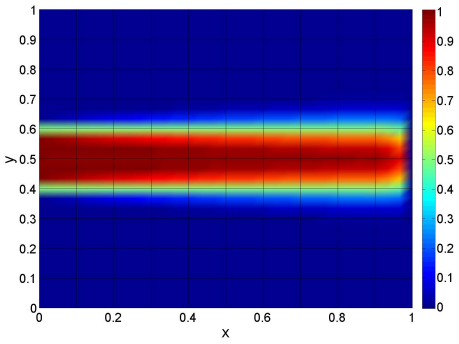

(f) $\alpha = 0.0001$, stabilized quadrilaterals with $p = 3$, $Pe_c = 50$

Figure 4.17

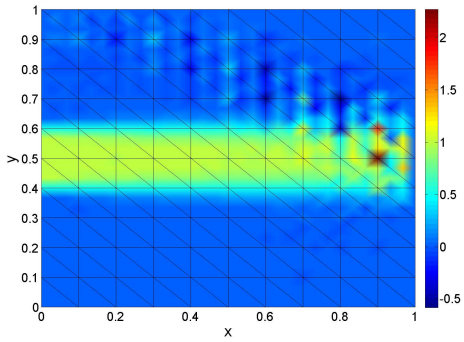

(g) $\alpha = 0.00001$, non-stabilized structured tringulars with $p = 3$, $Pe_c = 50$

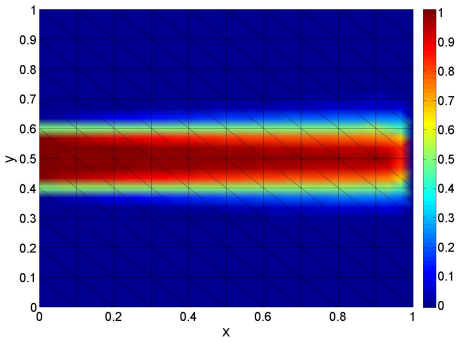

(h) $\alpha = 0.00001$, stabilized structured tringulars with $p = 3$, $Pe_c = 50$

Figure 4.17: DG solution, $p = 3$, convection-dominated regime, quadrilaterals elements are with 10 elements on each side, structured triangulars with 20 elements on each side, and unstructured tringulars with total of 328 elements. The original mesh is represented within each figure

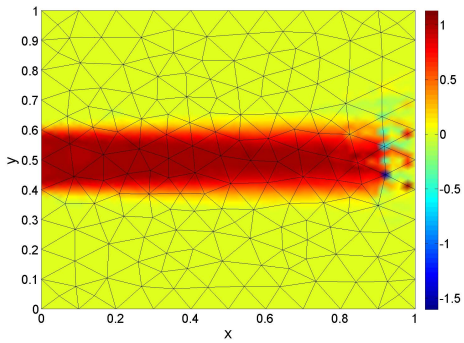

(a) $\alpha = 0.01$, non-stabilized unstructured tringulars with $p = 4$, $Pe_c = 57$

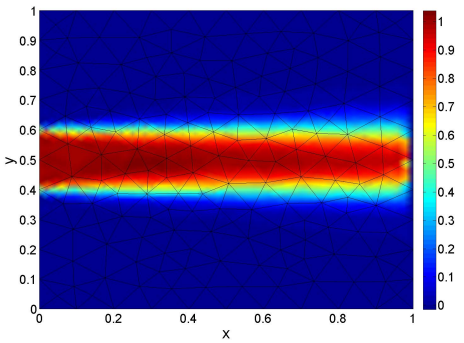

(b) $\alpha = 0.01$, stabilized unstructured tringulars with $p = 4$, $Pe_c = 57$

Figure 4.18

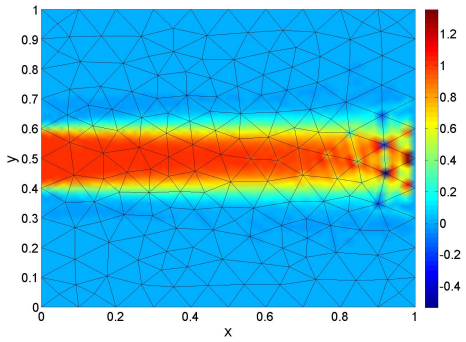

(c) $\alpha = 0.001$, non-stabilized unstructured tringulars with $p = 4$, $Pe_c = 57$

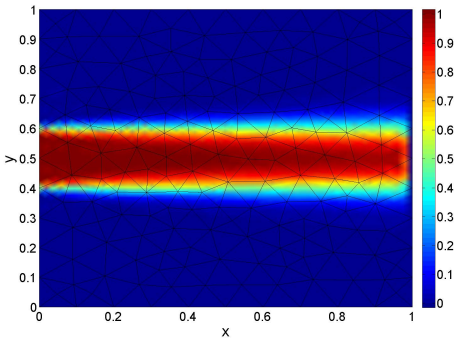

(d) $\alpha = 0.001$, stabilized unstructured tringulars with $p = 4$, $Pe_c = 57$

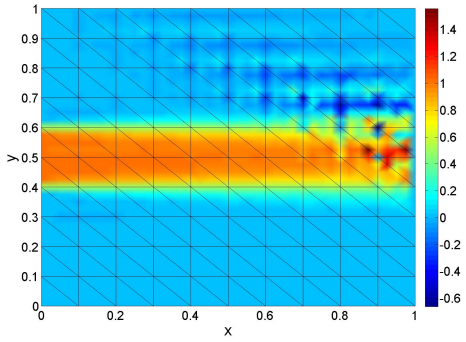

(e) $\alpha = 0.0001$,non-stabilized structured tringulars with $p = 4$, $Pe_c = 50$

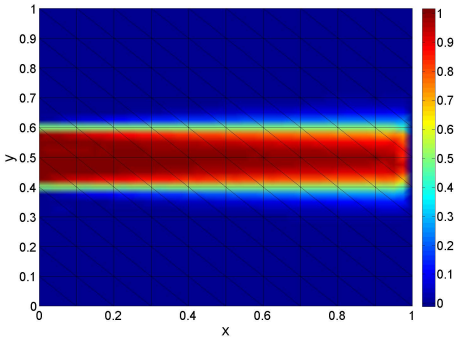

(f) $\alpha = 0.0001$, stabilized structured tringulars with $p = 4$, $Pe_c = 50$

Figure 4.18

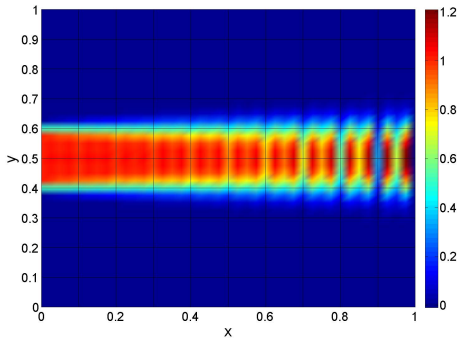

(g) $\alpha = 0.00001$,non-stabilized quadrilaterals with $p = 4$, $Pe_c = 50$

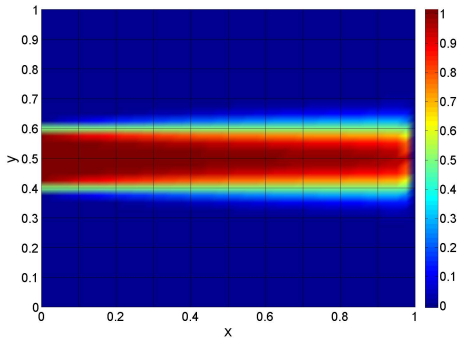

(h) $\alpha = 0.00001$, stabilized quadrilaterals with $p = 4$, $Pe_c = 50$

Figure 4.18: DG solution, $p = 4$, convection-dominated regime, quadrilaterals elements are with 10 elements on each side, structured triangulars with 20 elements on each side, and unstructured tringulars with total of 328 elements. The original mesh is represented within each figure

4.3 An Application Based Problem: Fuel Concentration in a Combustor

In this section, an application based example has been presented. This example models the jet diffusion flame in a combustor. The parameters of the problem have been taken as the ones in a study of the same problem within (37) to compare the results. The problem is governed by transient nonlinear reaction-convection-diffusion equations which was presented in section (4.1) by equation 4.1.

Considering the equation 4.1 for our problem, the variable u represents the concentration of fuel in the domain, the coefficient $\boldsymbol{a}$ is the convection velocity, and k the diffusion coefficient which are all taken as constant, and the source term is assumed as $f = 0$. The term $R(u)$ is an Arrhenius type nonlinear reaction given by,

$$R(u;\mu) = Au(c-u)\,e^{-E/(d-u)} \tag{4.12}$$

where c and d are known constants and the system parameters defined as $\mu = (\ln A, E)$ can vary within the parameter domain $\mathcal{D} : [5, 7.25] \times [0.05, 0.15]$ according to (37). From a physical point of view, u represents fuel concentration, whereas $c - u$ is the

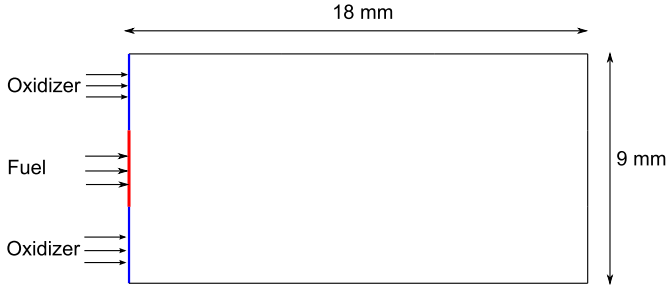

Figure 4.19: The domain for the modeled fuel concentration problem

concentration of the oxidizer. The parameters A and E are usually estimated from experimental data. Figure 4.19 shows the 2D combustor domain.

A flow velocity of $0.2\,(m/s)$ has been considered in x direction, the diffusion coefficient taken as $k = 5 \times 10^{-6}\left(m^2/s\right)$. The fixed Arrhenius parameters are $c = 0.2$ and $d = 0.24$, and the system parameters set to $\mu = (6.4318, 0.1091)$. On the left side of the boundary (at the Dirichlet boundary) as shown in figure 4.19, the value of u denoted by u_D is set to c at the fuel inflow, and set to 0 at the oxidizer inflow. On the right side of the domain two types of conditions have been considered, either zero Dirichlet or zero Neumann boundary conditions.

Considering zero Dirichlet boundary conditions on the right side of the domain, results for CG and DG solution of the problem have been represented in figure 4.20 in a steady case. It's observed that in CG non-stabilized case there are spurious oscillations which imply the need for stabilization as shown on the left column of the same figure. Regarding the DG, for comparatively small values of penalty coefficient ($\alpha = 1e-8$) results seem to perform in continuous space and hence experiencing the same stability problems as in CG case. On the other hand, for larger values of penalty coefficient ($\alpha = 5e-5$ or $\alpha = 1e-4$) but still not very close to the critical value ($\alpha_c = 0.5$), in the non-stabilized results the jumps are quite visible in the figures whereas the stabilized DG solution perform better results and well agreeing with the stabilized CG case. Note that the reason for having small values of α can be explained by looking back into our DG formulation (3.40), and considering the portion k/δ in the diffusion continuity term with $\delta = \alpha h$. Accordingly for small values of diffusion coefficient here ($k = 5e-6$), the value of α need to be such that the appropriate penalty parameter (δ) value is ensured with respect to the continuity terms. Of course the values of α need to avoid over-penalization by very small values, and also need to ensure appropriate results by

taking values not very close to critical values, also the importance of the mesh size in results should be noticed.

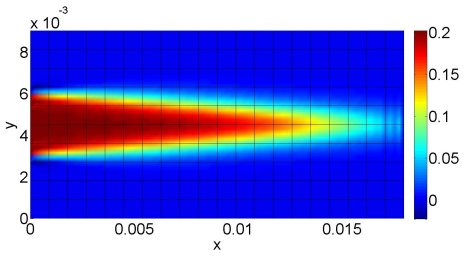

(a) CG, $p = 4$, non-stabilized

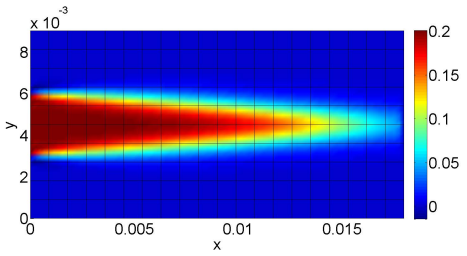

(b) CG, stabilized

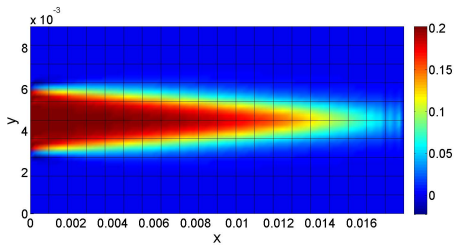

(c) DG, $p = 4$, non-stabilized, $\alpha = 1e - 8$

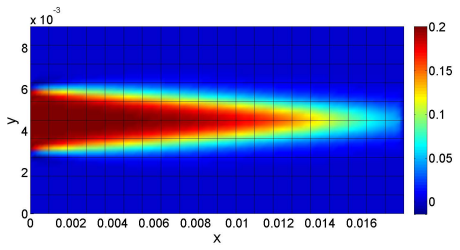

(d) DG, $p = 4$, stabilized, $\alpha = 1e - 8$

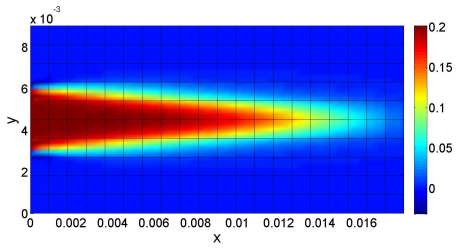

(e) DG, $p = 4$, non-stabilized, $\alpha = 5e - 5$

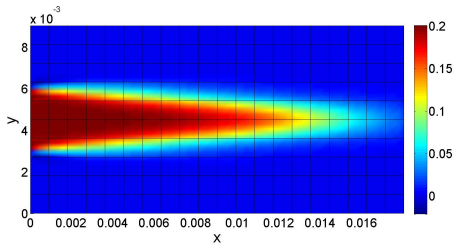

(f) DG, $p = 4$, stabilized, $\alpha = 5e - 5$

Figure 4.20

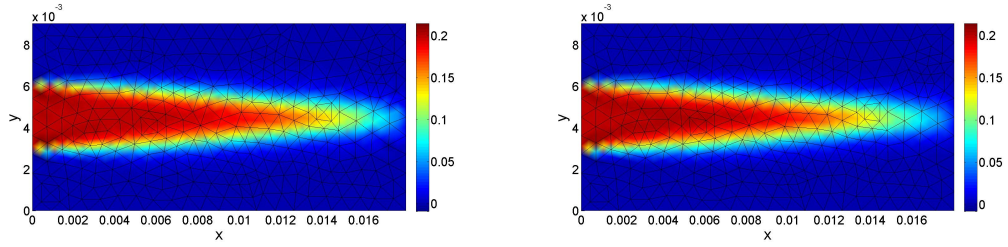

(g) DG, $p = 2$, non-stabilized, $\alpha = 1e-4$ **(h)** DG, $p = 2$, stabilized, $\alpha = 1e-4$

Figure 4.20: Fuel concentration in a steady case (nonlinear RCD equation), zero Dirichlet BC on right boundary, comparison of non-stabilized and stabilized CG and DG solutions, quadrilaterals with $[20 \times 10]$ elements and $p = 4$, and unstructured triangulars with $n_{tot} = 664$ elements and $p = 2$. Note: original mesh has been represented.

Now let us consider the transient nonlinear case with $u_0 = 0$ at time $t = 0$, and considering a Neumann boundary condition on the right side of the boundary. In figure 4.21, the results using CG and DG solution of the problem have been represented. In these figures the results after the steady state time denoted by (t_s) have been shown. Also in the same figures, the time step has been denoted by δt. The DG results are all stabilized, in order to make the formulation non-sensitive to the penalty parameter while still considering values of α that would avoid performing our DG solution in continuous space. According to the results it is observed that for two different meshes with different degrees of approximations, and also different α values the obtained results are well agreeing. These application based results, following previously obtained results and discussions, may indicate the benefits of stabilization in DG formulations and specifically, as in our study, the convection dominated CDR problems.

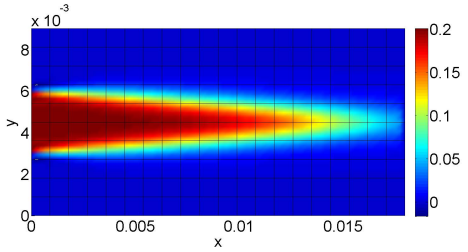

(i) CG, $p = 4$, stabilized, transient case, $t_s = 0.32\,(s)$ with $\delta t = 0.01$

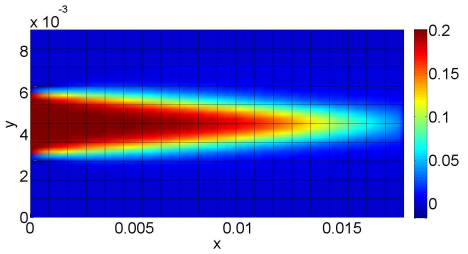

(j) DG, $p = 4$, stabilized, $\alpha = 1e-5$, transient case, $t_s = 0.36\,(s)$ with $\delta t = 0.01$

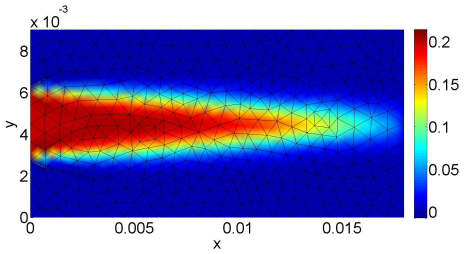

(k) DG, $p = 2$, non-stabilized, $\alpha = 1e-4$, transient case, $t_s = 0.33\,(s)$ with $\delta t = 0.01$

Figure 4.21: Fuel concentration in a transient case (transient nonlinear RCD equation), zero Neumann BC on right boundary, stabilized DG solutions, quadrilaterals with $[20 \times 10]$ elements and $p = 4$, and unstructured triangulars with $n_{tot} = 664$ elements and $p = 2$. Note: original mesh has been represented.

5

Conclusions

A stabilized Discontinuous Galerkin (DG) formulation was proposed for Convection Diffusion Reaction (CDR) equations using high order approximations. A three field hybrid approach was used in order to derive our DG formulation. The resulting DG formulation turns out to be very classical; the only difference is in the term that enforces continuity in the direction of convection velocity when diffusion goes to zero. The developed DG formulation recovers the Interior Penalty (IP) method, preserves adjoint consistency, and its flux continuity terms are derived naturally and without using the common ad-hoc approaches.

Some simple numerical examples were conducted using the developed DG formulation for CDR problem and in particular in the case of convection-dominated regime, which were compared to the Continuous Galerkin (CG) results obtained for the same problem. It was shown that the results obtained using the DG method are strongly dependent on the penalty parameter (δ). There were some interesting observations which were concluded according to the proposed DG formulation and were verified by our results. Suppose $\delta = \alpha h$, when $\alpha \to 0$ while k is fixed and considering Peclet (Pe) number as $Pe < 1$ or $Pe > 1$ (convection-dominated case), the formulation will enforce, strongly, the continuity. In this case it was observed that the same stability problems as in the case of continuous Galerkin are encountered which implies that the DG results are performing in continuous space. Whereas for critical values of penalty parameter when $\alpha \to \alpha_c$ (with an interpretation of $\alpha_c = 0.5$) excessive continuity will be enforced in the direction of convection velocity which is manifested by bigger jumps across the

element boundaries. These results indicate the strong dependence of the DG results on penalty parameter and also the difficulties in determining an appropriate value for it.

To overcome these problems, a stabilization of the DG method was proposed i.e. using the same stabilization strategy for discontinuous interpolations as for continuous ones. The proposed stabilized formulation was motivated from the variational multi-scale (VMS) concept. From the proposed numerical examples, the benefits of adding stabilization to the original discontinuous Galerkin formulation were shown. Without this term, the solution exhibits a strong dependence on the parameter α that enforces weak continuity of the unknown. Adding the stabilization term, the solution is virtually insensitive to this parameter. Our numerical examples in different cases and using linear to higher orders of approximation ($p = 1, \cdots, 4$) indicate that the stabilized DG results for different values of α perform very closely which verifies the above conclusions. From the analytical point of view, these results are explained by the dependence of the stability and convergence bounds on α, which explode as continuity of the unknown is excessively enforced and no additional stabilization is added.

Finally, an application based problem was presented in which the fuel concentration was computed in a combustor. The governing transient nonlinear reaction-convection-diffusion equations were derived considering parameters for convection-dominated regime and by considering the reaction term modelled as an Arrhenius type nonlinear function. The problem was numerically solved using the proposed stabilized DG method and the derived DG results were compared to the computed CG results for the same problem. In the end, the same discussions and conclusions explained above were clearly observed and verified for this application based example as well as the other proposed examples.

Bibliography

[1] F. Bassi, and S. Rebay. **A high-order accurate discontinuous finite element method for the numerical solution of the compressible Navier-Stokes equations**. *J. Comput. Phys. 131 (2), 267-279*, 1997. 4, 21, 31

[2] T.J.R. Hughes, G. Engel, L. Mazzei, M.G. Larson. **A comparison of discontinuous and continuous Galerkin methods based on error estimates, conservation, robustness and efficiency**. *in: B. Cockburn, G.E. Karniadakis, C.-W. Shu (Eds.), Discontinuous Galerkin Methods: Theory, Computation and Applications, Springer-Verlag*, 2000. 5, 31

[3] P. Bochev, T.J.R. Hughes, and G. Scovazzi. **A Multiscale Discontinuous Galerkin Method**. *Siam J. Numer. Anal. 44 (4), 14201440*, 2006. 4, 31

[4] F. Brezzi, G. Manzini, D. Marini, P. Pietra, and A. Russo. **Discontinuous Galerkin approximations for elliptic problems**. *Numerical methods in PDEs, 16 (4), 365378*, 2000. 4, 31

[5] C. Dawson. **The P^{k+1}-S^k local discontinuous Galerkin method for elliptic equations**. *Siam J. Numer. Anal. 40 (6), 21512170*, 2003. 4, 31

[6] T. J. R. Hughes, A. Masud, and J. Wan. **A stabilized mixed discontinuous Galerkin method for Darcy flow**. *Comp. Meth. Appl. Mech. Enrgr, 195 (25-28), 3347-3381*, 2006. 4, 31

[7] B. Cockburn, G. Karniadakis and C.-W. Shu. **The development of discontinuous Galerkin methods, in Discontinuous Galerkin Methods: Theory, Computation and Applications**. *B. Cockburn, G. Karniadakis and C.-W. Shu, editors, Lecture Notes in Computational Science and Engineering, Springer, 11 3-50, Part I: Overview*, 2000. 22

[8] F. Brezzi, B. Cockburn, L.D. Marini,, and E. Süli. **Stabilization mechanisms in Discontinuous Galerkin finite element methods**. *Comput. Methods Appl. Mech. Eng., 195, 32933310*, 2002. 31

[9] Douglas N. Arnold, Franco Brezzi, Bernardo Cockburn, and L. Donatella Marini. **Unified analysis of Discontinuous Galerkin methods for elliptic problems**. *SIAM J. NUMER. ANAL. 39 (5), 17491779*, 2002. 4, 5, 21, 31

[10] T.J.R. Hughes, G.R. Feijóo, L. Mazzei, and J.-B. Quincy. **The Variational Multiscale Method a paradigm for computational mechanics**. *Computer Methods in Applied Mechanics and Engineering, 166, 324*, 1998. 12, 16

[11] T. J. R. Hughes and A. N. Brooks. **A multidimensional upwind scheme with no crosswind diffusion**. *in T. J. R. Hughes, editor, FEM for convection dominated flows, New York, . ASME*, 1979. 3

[12] D. Kelly, S. Nakazawa, O. Zienkiewicz, and J. Heinrich. **A note on upwinding and anisotropic balancing dissipation in finite element approximations to convective diffusion problems**. *International journal for numerical methods in engineering, 15, 17051711*, 1980. 3

[13] A. N. Brooks, and T. J. R. Hughes. **Streamline upwind/petrov-galerkin formulations for convection dominated flows with particular emphasis on the incompresible Navier-Stokes equations**. *Computer Methods in Applied Mechanics and Engineering, 32, 199259*, 1982. 3

[14] T. J. R. Hughes, L. P. Franca, and G. M. Hulbert. **A new finite element formulation for computational fluid dynamics: VIII. The galerkin/least-squares method for advective-diffusive equations**. *Computer Methods in Applied Mechanics and Engineering, 73(2), 173189*, 1989. 3

[15] T.J.R. Hughes, L.P. Franca, M. Balestra. **A new finite element formulation for computational fluid dynamics: V. Circumventing the BabuskaBrezzi condition: a stable PetrovGalerkin formulation of the Stokes problem accommodating equal-order interpolations**. *Methods Appl. Mech. Engrg. 59, 8599*, 1986. 3

[16] I. Christie, D.F. Griffiths, A.R. Mitchell, O.C. Zienkiewicz. **Finite element methods for second order differential equations with significant first derivatives**. *Int. J. Numer. Methods Eng. 10, 1389-1396*, 1976. 2

[17] J.C. Heinrich, P.S. Huyakorn, O.C. Zienkiewicz, A.R. Mitchell. **An 'upwind' finite element scheme for two-dimensional convective transport equation**. *Int. J. Numer. Methods. Eng. 11 131-143*, 1977. 2

[18] M. Tabata. **A finite element approximation corresponding to the upwind finite differencing**. *Mem. Numer. Math. 4 47-63*, 1977. 2

[19] J. Douglas and J. Wang. **An absolutely stabilized finite element method for the Stokes problem**. *Mathematics of computation, 52, 495508*, 1989. 3

[20] F. Brezzi, M. Bristeau, L. Franca, M. Mallet, and G.Rogé. **A relationship between stabilized finite element methods and the Galerkin method with bubble functions**. *Computer Methods in Applied Mechanics and Engineering, 96, 117129*, 1992. 3

[21] C. Baiocchi, F. Brezzi, and L. Franca. **Virtual bubbles and Galerkin/least-squares type methods (Ga.L.S)**. *Computer Methods in Applied Mechanics and Engineering, 105, 125141*, 1993. 3

[22] L. Franca and C. Farhat. **Bubble functions prompt unusual stabilized finite element methods**. *Computer Methods in Applied Mechanics and Engineering, 123, 299308*, 1995. 3

BIBLIOGRAPHY

[23] L. Franca and A. Russo. **Deriving upwinding, mass lumping and selective reduced integration by residual-free bubbles**. *Applied Mathematics Letters, 9(5), 253276*, 1996. 3

[24] T.J.R. Hughes. **Multiscale phenomena: Green's functions, the Dirichlet-to-Neumann formulation, subgrid scale models, bubble and origin of stabilized methods**. *Comput. Methods Appl. Mech. Engrg. 127 387-401*, 1995. 3, 9, 12

[25] P. Castillo. **Performance of discontinuous Galerkin methods for elliptic PDEs**. *SIAM J. Sci. Comput., 24, 524547*, 2002. 4

[26] J. Douglas, Jr., and T. Dupont. **Interior penalty procedures for elliptic and parabolic Galerkin methods**. *in Computing Methods in Applied Sciences (Second Internat. Sympos., Versailles, 1975), Lecture Notes in Phys. 58, Springer, Berlin, 207216*, 1976. 4, 21, 31

[27] B. Cockburn and C.-W. Shu. **The local discontinuous Galerkin method for time-dependent convection-diffusion systems**. *SIAM J. Numer. Anal., 35, 24402463*, 1998. 4, 21, 31

[28] R. Codina. **Stabilized finite element approximation of transient incompressible flows using orthogonal subscales**. *Computer Methods in Applied Mechanics and Engineering, 191(39-40, 42954321*, 2002. 15, 17

[29] R. Codina. **Comparison of some finite element methods for solving the diffusion-convection-reaction equation**. *Computer Methods in Applied Mechanics and Engineering, 156:185210*, 1998. 4, 18

[30] J. Principe, R. Codina. **On the stabilization parameter in the subgrid scale approximation of scalar convectiondiffusionreaction equations on distorted meshes**. *Comput. Methods Appl. Mech. Engrg. 199, 13861402*, 2010. 19

[31] R. Codina, E. Oate, M. Cervera. **The intrinsic time for the streamline upwind/ PetrovGalerkin formulation using quadratic elements**. *Comput. Methods Appl. Mech. Engrg. 94, 239262*, 1992. 18

[32] W. Reed, T. Hill. **Triangular mesh methods for the neutron transport equation**. *In Tech. Report LA-UR-73-479, Los Alamos Scientific Laboratory*, 1973. 21

[33] J. Peraire, P.-O. Persson. **The Compact Discontinuous Galerkin (CDG) method for elliptic problems**. *SIAM J. Sci. Stat. Comput. 30 (4), 1806-1824*, 2008. 21

[34] A. Ern, A. Stephansen, P. Zunino. **A Discontinuous Galerkin method with weighted averages for advection-diffusion equations with locally vanishing and anisotropic diffusivity**. *IMA J Numer Anal, 29(2): 235-256*, 2009. 30

[35] Markus Bause. **Performance of Stabilized Higher-Order Methods for Nonstationary Convection-Diffusion-Reaction Equations**. *Lecture Notes in Computational Science and Engineering, 81, 11-19*, 2010. 20

[36] R. Codina, E. Oñate, M. Cervera. **The intrinsic time for the streamline upwind/ PetrovGalerkin formulation using quadratic elements**. *Comput. Methods Appl. Mech. Engrg. 94, 239262*, 1992. 20

[37] D. Galbally, K. Fidkowski, K. Willcox, O. Ghattas. **Nonlinear model reduction for uncertainty quantification in large-scale inverse problems**. *Int. J. Numer. Meth. Engng, 81, 15811608*, 2010. 65